Structure and exhumation of the Cap des Trois Fourches basement rocks (Eastern Rif, Morocco)

Ali Azdimousa, Antonio Jabaloy-Sánchez, Philippe Münch, J. M Martínez-Martínez, Guillermo Booth-Rea, Mercedes Vázquez-Vílchez, Lahcen Asebriy, Jacques Bourgois, Francisco González-Lodeiro

Accepted Manuscript

Structure and exhumation of the Cap des Trois Fourches basement rocks (Eastern Rif, Morocco)

A. Azdimousa, A. Jabaloy-Sánchez, P. Münch, J.M. Martínez-Martínez, G. Booth-Rea, M. Vázquez-Vílchez, L. Asebriy, J. Bourgois, F. González-Lodeiro

PII: S1464-343X(18)30300-5

DOI: 10.1016/j.jafrearsci.2018.09.018

Reference: AES 3330

To appear in: *Journal of African Earth Sciences*

Received Date: 30 January 2017

Revised Date: 31 August 2018

Accepted Date: 25 September 2018

Please cite this article as: Azdimousa, A., Jabaloy-Sánchez, A., Münch, P., Martínez-Martínez, J.M., Booth-Rea, G., Vázquez-Vílchez, M., Asebriy, L., Bourgois, J., González-Lodeiro, F., Structure and exhumation of the Cap des Trois Fourches basement rocks (Eastern Rif, Morocco), *Journal of African Earth Sciences* (2018), doi: https://doi.org/10.1016/j.jafrearsci.2018.09.018.

Structure and exhumation of the Cap des Trois Fourches basement rocks (Eastern Rif, Morocco)

Azdimousa, A.[1], Jabaloy-Sánchez, A.[2], Münch, P.[3], Martínez-Martínez, J.M.[2,4], Booth-Rea, G.[2,4], Vázquez-Vílchez, M.[5], Asebriy, L.[6], Bourgois, J.[7], González-Lodeiro, F.[8]

1 Faculté Pluridisciplinaire de Nador & Laboratoire des Géosciences Appliquées, Faculté des Sciences, Université Mohammed I, Oujda, Morocco.

2 Departamento de Geodinámica, Universidad de Granada, Granada, Granada, (Spain).

3 Géosciences Montpellier, Université de Montpellier, Campus Triolet CC060, place Eugene Baitaillon, 34095 Montpellier cedex, France.

4 Instituto Andaluz de Ciencias de la Tierra, UGR-CSIC, Avda. de las Palmeras, 18100 Armilla, Granada, (Spain)

5 Departamento de Didáctica de las Ciencias Experimentales, Facultad de Ciencias de la Educación, Universidad de Granada, Granada, Spain)

6 Institut Scientifique, B.P. 703, Université Mohammed V, Agdal-Rabat, Morocco.

7 Université Pierre et Marie Curie - Paris 6. Institut des Sciences de la Terre Paris (iSTeP) - UMR 7193 UPMC-CNRS Case 124, Tour 46-00, 3 ème étage, 4, place Jussieu, 75252 Paris Cedex 5, France

8 Instituto Geológico y Minero de España, Ríos Rosas 23, 28003 Madrid, Spain

Abstract

The Cap des Trois Fourches (Eastern Rif, northern Morocco) metamorphic basement exposes two major tectonic units, namely the Taïdant unit underthrusting the overlying Tarjât tectonic unit. The Tarjât tectonic unit is composed of metamorphic rock originating from detrital material. This upper Tarjât tectonic unit exhibits: (1) orthogneiss bodies being Paleozoic in age and (2) evidences showing a retromorphose during the Alpine orogenesis. U-Pb SHRIMP zircon geochronology from the orthogneiss bodies has yielded Sakmarian (Early Permian) ages for the intrusion of their protoliths. The lower Taïdant unit is formed of green and brown shales associated with quartzite beds. A Mesozoic age is commonly accepted for this unit.

The internal structure of the Tarjât tectonic unit consists in km-scale folds trending ENE-WSW with an up-dip direction towards the SE. This compressional deformational stage was superimposed on internal thrust sheets controlled by ductile shear zones with a SW-vergent transport sense. The lower Taïdant unit shows conspicuous bedding associated with a penetrative foliation outlining a monocline structure dipping gently towards the NW. The major ductile-brittle detachment fault bounding the upper Tarjât tectonic unit from the lower Taïdant unit –i.e. the local basement– exhibits evidences for a top-to-the-west sense of motion. We assume that this specific fault is the prolongation into the Cap des Trois Fourches area of the extensional detachment previously described in the Temsamane area. Therefore, this low angle detachment fault is a major tectonic element extending hundreds of km through the Eastern Rif. We postulate that this major detachment roots deep in the Eastern Rif basement. This detachment is cut at the surface by the Nekor normal-sinistral strike-slip fault that separates thin 24-32 km thick metamorphic Eastern Rif crust from the 50-55 km thick crust of the western Rif. This transtensive fault system exhumes the Rif middle crust, represented by the Temsamane massif units, along the Nekor sinistral STEP boundary at the southern edge of the Betic-Rif subduction system.

Keywords: Rif Chain, Cap des Trois Fourches, ductile-brittle detachment fault, U-Pb SHRIMP zircon geochronology

1. - Introduction

The Eastern Rif Chain (Northwest Africa, Fig. 1) is characterized by very low- to low-grade metamorphic terranes derived from the Mesozoic Maghrebian palaeomargin cropping out in different isolated sectors along the Mediterranean coast (Frizon de

Lamotte, 1985; Frizon de Lamotte et al., 1991; Azdimousa et al., 2007; Chalouan et al., 2008; Jabaloy et al., 2015). It notably includes the Temsamane area, the Cap des Trois Fourches and the Khebaba massif (Frizon de Lamotte, 1985; Frizon de Lamotte et al., 1991; Azdimousa et al., 2007; Negro et al., 2008; Booth-Rea et al., 2012; Jabaloy et al., 2015) (Figs. 1 and 2). The sequences of these areas include metapelitic Paleozoic rocks covered by Triassic greenschists and Jurassic to early Cretaceous marbles and metapelites (Frizon de Lamotte, 1985; Frizon de Lamotte et al., 1991; Azdimousa et al., 2007; Negro et al., 2008; Booth-Rea et al., 2012; Jabaloy et al., 2015). Those rocks are characterized by LT-IP Alpine metamorphic conditions (Negro, 2005; Negro et al., 2007; Jabaloy et al., 2015), and by penetrative Alpine ductile deformations. Most of the rocks also were exhumed by a ductile-brittle extensional detachment (see Azdimousa et al., 2007; Booth-Rea et al. 2012; Jabaloy et al., 2015). At the present day, those metamorphic outcrops are isolated, making their mutual correlation difficult to disentangle the first order structure of the area that is a basic key point to understand the evolution of the North Africa palaeomargin.

One of the aforementioned outcrops occurs in the Cap des Trois Fourches sector (Figs. 2 and 3), where scarce detailed studies have been performed (Guillemin et al., 1983; García-Dueñas et al., 1995; Sánchez-Gómez, 1996; Michard et al., 2008; Negro et al., 2008). The rocks of this specific massif have been tentatively correlated with those of the Internal Rif (García-Dueñas et al., 1995; Sánchez-Gómez, 1996) or the uppermost and most metamorphosed of the Temsamane metamorphic units: the Ras Afraou unit (Michard et al., 2008; Negro et al., 2008).

Our main aim is to establish the structure of the low-grade metamorphic outcrops of the Cap des Trois Fourches sector in order to determine their tectonic evolution and correlation with the Rifian structures. In order to do so we carried a detailed microtectonic analysis combined with $^{40}Ar/^{39}Ar$ ages on white micas and SHRIMP U-Pb dating on zircons.

2.-Tectonic setting

The Rif Chain is an Alpine mountain belt bordering northern Morocco (Fig. 1) that in union with the Betic Chain belt in southern Spain form the Betic–Rif orogen (e.g., Booth-Rea et al., 2005; Chalouan et al., 2008; Platt et al., 2013, and references therein). This orogen was formed during the westward drifting of the Alborán domain (Andrieux et al., 1971; Bourgois, 1977; Balanyá and García-Dueñas, 1987), at the same time as the African and Eurasian plates converged (e.g., Chalouan and Michard, 2004; Jolivet et al., 2003) during the Oligocene-Miocene times (Chalouan and Michard, 2004; Chalouan et al., 2008).

The tectonic model for these movements in the Western Mediterranean area is controversial, although most of them involve the westwards roll back of a SE-dipping slab of Tethys lithosphere below the Alborán domain (i.e. Rosenbaum et al., 2002; Faccenna et al., 2004; Booth-Rea et al., 2007; Carminati et al., 2012; Chertova et al., 2014), while others authors propose delamination or convective removal of the subcontinental mantle lithosphere (Calvert et al., 2000; Platt et al., 1998; Seber et al., 1996). Seismic studies have delimited a SE-dipping high-velocity slab within the upper mantle beneath the Gibraltar Arc (i.e. Bezada et al., 2013; Palomeras et al., 2014; Thurner et al., 2014; Mancilla et al., 2015; Villaseñor et al., 2015) that together with geochemical data of volcanic rocks in the region (Duggen et al., 2008; Varas-Reus et al., 2017) and the volcanic arc structure of the East Alboran basin (Booth-Rea et al., in press) favours the subduction/roll-back models. However, delamination of the subcontinental lithosphere at the edges of the subduction system in the Betics and Rif, coeval to slab rollback, is supported by the geochemical evolution of volcanism (Duggen et al., 2003), by tectonic analysis (Martínez-Martínez et al., 2006), and by receiver function data that show a missing orogenic root under parts of the Betics and the Eastern Rif (Thurner et al., 2014; Mancilla et al., 2015). Delamination occurred under the continental orogenic crust inboard of Subduction Transfer Edge Propagator boundaries (STEP, Govers and Wortel, 2005) at the northern and southern edges of the Betic-Rif orogen (Mancilla et al., 2015).

From the Mediterranean coast towards the south, three main structural domains compose the Rif belt (Fig. 1):

i) Internal Rif or Alborán Domain that is an allochthonous terrain mainly composed by metamorphic and sedimentary rocks exhibiting ages ranging from Paleozoic to Paleogene.

ii) Maghrebian Flysch units thrusted southward as tectonic sheets mainly formed of Mesozoic-Cenozoic turbidites. They are commonly interpreted as rocks originating from the main suture of the Tethys Ocean (Durand-Delga et al., 2000). Bourgois (1980 a, b) has inferred that this main suture is located north of the Internal Zones in the Betic Chain.

iii) External Rif formed of Mesozoic to Cenozoic sediments and metasediments, and interpreted as the North African passive margin of the Tethys Ocean.

Traditionally, the External Rif rocks have been grouped into three main zones: the Prerif, the Intrarif, and the Mesorif zones (Suter, 1980a, b). The Prerif zone is the outermost zone of the External Rif and is located to the south. It comprises a frontal fold-and-thrust belt that deforms thin Jurassic and Lower Cretaceous successions detached from the Paleozoic basement of the Variscan Western Moroccan Meseta (“Rides Prérifaines”, see Michard, 1976; Ben Yaïch, 1991; Favre, 1992). The “Rides Prérifaines” are overlain by an olistostromic complex formed of Paleozoic to Cenozoic blocks in a matrix of Tortonian marls ("Nappe Prérifaine", Levy and Tilloy, 1952; Vidal, 1971; Leblanc, 1975-1979; Bourgois, 1977; Suter, 1980a, b; Feinberg, 1986; Kerzazi, 1994).

The Mesorif zone is formed of allochthonous units with Triassic to Paleogene successions thrusting over autochthonous or para-autochthonous successions culminating with Middle-Upper Miocene turbidites and olistostromes. Those lithological successions are thought to be deposited in proximal areas of the African paleomargin (e.g. Chalouan et al., 2008). However, recently Benzaggagh et al. (2014) have proposed the existence of ophiolitic massifs indicating the opening of ocean-floor basins within the Mesorif domain. In the eastern Rif, those Mesorif units correspond to the Temsamane units that underwent ductile deformations and IP-IT metamorphism during Alpine times (see Azdimousa et al., 2007, Jabaloy et al., 2015, and references therein).

The Intrarif zone includes the distal units derived from the African paleomargin. These units crop out immediately beneath the Maghrebian Flyschs and Internal Rif and are characterized by a thick accumulation of sediments with ages ranging from Lower Jurassic to Cretaceous. These sediments underwent ductile deformations that developed under diagenetic to anchizone conditions (Andrieux, 1971; Asebriy, 1994; Asebriy et al., 2003; Azdimousa et al., 1998, 2003, 2007; Vazquez et al., 2013). The Mesorif units include the Ketama unit, overlain by the partly detached Tanger unit, and the Aknoul nappe, totally detached and containing the Upper Cretaceous-Eocene succession.

Asebriy et al. (1987) have defined the Subrif zone located north of the Prerif zone that includes the Intrarif and Mesorif units as defined by Durand-Delga et al. (1962) and (Suter, 1980a,b). In the Eastern Rif (Fig. 2), the External Rif includes three main sets of tectonic units. From bottom to top, it includes: the Temsamane fold-and-thrust stack, the Tanger-Ketama unit, and the Aknoul unit.

The lithological sequence of the Temsamane fold-and-thrust stack begins with dark Paleozoic schists covered by Triassic greenschists and Jurassic marbles. Continuing up section, whitish Berriasian–Barremian phyllites and shales alternate with marbles, and they are covered by dark Aptian–Early Albian phyllites and shales alternating with quartzites (Frizon de Lamotte, 1985; Frizon de Lamotte et al. 1991; Azdimousa et al., 2007). The rocks are deformed by isoclinal to tight folds with N70ºE strikes and SSE vergences (see Azdimousa et al., 2007; Jabaloy et al., 2015). Ductile shear zones bound several fold-nappes (Jabaloy et al., 2015). The metamorphic P-T conditions increase towards the NW, with late diagenesis reaching epizone at chlorite-illite conditions in the lowermost fold-nappe. The early Cretaceous metapelites in the intermediate Temsamane fold-nappes, and the Paleozoic schists in both the Ras Afraou and Khebaba units at the top of the stack, exhibit chloritoid bearing facies (Frizon de Lamotte, 1987; Negro, 2005; Negro et al., 2007).

Negro (2005), Negro et al. (2007), Jabaloy et al. (2015), have estimated the PT metamorphic conditions of the rocks in the uppermost Temsamane unit (Ras Afraou unit) at 7–8 kbars and 350 ± 30 °C. $^{40}Ar/^{39}Ar$ radiometric analyses on white micas have yielded ages ranging from 23 to 8 Ma (Monié et al., 1984; Negro et al., 2008; Jabaloy et al., 2015). Negro et al. (2008) and Jabaloy et al. (2015) have proposed the older Oligocene ages correspond to the metamorphic peak during subduction, and those of the Middle to Late Miocene date the cooling during extensional exhumation of the rocks.

The exhumation of the Temsamane metamorphic rocks took place along a major extensional detachment with tectonic transport towards the WSW that is the so-called Temsamane detachment, separating the Temsamane fold-and-thrust stack in the footwall from the Tanger–Ketama and Aknoul units in the hanging wall (Booth-Rea et al., 2012). In turn, the sedimentary Mesozoic cover of the Eastern Moroccan Meseta or their prolongation as the Middle Atlas underthrusts the metamorphic Temsamane fold-and-thrust stack. In contrast, the structure in the western Rif includes structurally higher rock units with the thick Jurassic marbles and Cretaceous slates of the Tanger-Ketama unit (see Vázquez et al., 2013) covering the ophiolitic bodies of the Central Rif (Benzaggagh et al., 2014; Amar et al., 2015), and, in turn, these rocks are overthrust by the Maghrebian Flysch units and the Internal Rif Alboran domain rocks.

Below the Rif Chain, the Moho shows strong differences in depth, ranging from more than 50 km below the western and central Rif to around 24 km below the eastern Rif. These two structural domains are separated by a steep transition zone (Mancilla et al., 2012, 2015; Díaz et al., 2016) located beneath the active Trougout-Nekor Fault-system. GPS data (Vernant et al., 2010; Pérouse et al 2010) and reorganization of the drainage networks (Barcos et al., 2014) have recorded the tectonic activity along this Trougout-Nekor fault system. This sinistral transtensional fault-system (Asebriy et al., 1993; Barcos et al., 2014; Poujol et al., 2014) accommodates most of the Present-day Western Rif belt displacement towards the WSW with respect to the stable Nubia (Poujol et al., 2014).

3. - Geology of the Cap des Trois Fourches area

The rocks of the Cap des Trois Fourches area extend along the Peninsula of Melilla, a North-South elongated cap on the southern border of the Alboran Sea (northeast of Morocco, Figs. 2 and 3) in an open antiform striking NE-SW: the Tarjât (also known as Taryat) anticline (Guillemin and Houzay, 1982). The normal left-handed Aït Lahsene fault bounds the NW limb of the Tarjât anticline (Ait Brahim, 1991; Morel, 1988; Azdimousa et Bourgois, 1993). García-Dueñas et al. (1995) and Michard et al., (2007) have recognized two tectonic units in the area:

i.- The Tarjât Unit (García-Dueñas et al., 1995) formed of chloritoid-bearing schists, phyllites, quartzites and marbles that underwent MP-LT metamorphism at around 7-9 kbars and 330-430 ºC during the Oligocene times (Negro et al., 2007, 2008). This unit overlies a detachment underlined by fragments of chloritites and "serpentinites" (García-Dueñas et al., 1995; Michard et al., 2007) that separates it from

ii.-the Taïdant Unit (García-Dueñas et al., 1995) formed of a thin sequence of shales and greywackes attributed to the Carboniferous.

García-Dueñas et al. (1995), and Negro et al. (2007, 2008) have previously described the grey chloritoid-bearing micaschists. These micaschists exhibit mineral associations including chlorite + phengite + quartz ± chloritoid ± paragonite ± kaolinite. The XMg from chloritoid shows values varying between: 0.08-0.14 (see Negro et al., 2007). They document 7-9 kbars and 330-430 ºC metamorphic P-T conditions for the grey schists at the base of the Tarjât unit. Also, they provide evidences for this metamorphism occurring during the Oligocene. The presence of kaolinite substantiates a retrometamorphic event that occurred during the late Miocene times. The previous studies of the metamorphic rocks discuss if they can be ascribed to the foreland of the Rif Chain (the Eastern Moroccan Meseta, Fernandez Navarro, 1911; Suter, 1980), to the Mesorif zone as the continuation of the outcrops of the Temsamane unit (Azdimousa et al., 2007; Michard et al., 2007; Booth-Rea et al., 2012), or to the Internal Rif (García-Dueñas et al., 1995; Negro et al., 2008).

Late Tortonian to Messinian sediments and volcanoclastics rocks, detached from the underlying metamorphic basement, crop out in the central part of the Melilla peninsula forming the Melilla Neogene basin (i.e. see Roger et al., 2000; Münch et al., 2001 and 2006 van Assen et al., 2006; and references therein). The northern and southern tips of the peninsula show two volcanic complexes. The northern Cap des Trois Fourches volcanic field exhibits rhyolites and rhyodacites with Tortonian ages (9.8 ± 3 Ma; Hernandez and Bellon, 1985). The southern Gourougou stratovolcano composed of Si-K rich igneous rocks spatially associated with Si-poor, Na-rich lavas was active from 6.69 to 3.37 Ma (Duggen et al., 2005).

4.-Description of rocks

Analytical methods for separation of minerals, chemical analysis, X-ray diffraction (XRD), $^{40}Ar/^{39}Ar$ dating on white micas, and SHRIMP U-Pb on zircons are described in the supporting information. The field work in the Cap des Trois Fourches area has revealed the presence of a major ductile fault separating the Tarjât Unit (García-Dueñas et al., 1995) from the underlying Taïdant tectonic unit formed of very low-grade metamorphic rocks and essentially outcropping at the south-eastern part of the massif.

4.1.- Stratigraphy of the Tarjât and the Taïdant unit

The stratigraphic sequence of the Tarjât unit begins with more than 350 m of grey chloritoid-bearing micaschists interlayered with quartzite layers including orthogneiss bodies, first described in this work.

Orthogneiss bodies outcrop in the northern part of the massif near the road to the lighthouse (Figs. 3, 4 and 5A). These are metric lens-shaped bodies several decimetres in thickness. These orthogneiss bodies show borders paralleling the main schistosity of the chloritoid-bearing schists. White layers rich in felsic minerals alternating with light grey layers of white mica and biotite (Fig. 5B) define prominent layering. K feldspar is clearly visible as centimetric porphyroblasts surrounded by the layering (Fig. 5B). The main mineral association includes K feldspar + quartz + muscovite + biotite + rutile.

The sequence follows up section with a ~10 meters thick quartzite-micaschist package covered by a brecciated dolomitised yellow marble discontinuous level. This marble always shows overlapping contacts over the above described sequence. The serpentinite bodies previously described in the area (see García-Dueñas et al., 1995; Michard et al., 2007) have been found to be chlorite-rich rocks (chloritites according to Michard et al., 2007). XRD data in sample CTF2 shows the presence of chlorite and quartz (Fig. 6). No serpentine mineral group exist in the bulk XRD patterns. If they exist, the abundance of serpentine mineral is less than 1%. Chlorite is the main phyllosilicate component identified from its characteristic reflections (14.18 Å, 7.08 Å, 4.72 Å and 3.54 Å) that differ from reflections of serpentine minerals (7.29 Å, 4.52 Å and 3.65 Å).

The lithological sequence of the underlying Taïdant Unit (García-Dueñas et al., 1995) consists of ~300 meters of green and brown shales interlayered with centimetric to decimetric levels of quartzites.

4.2.- Geochronology

Two samples from the orthogneiss bodies have been collected (AP3-F, C3F; see Fig. 3 for location). Samples were divided into two parts. The first one has been used for major, trace elements and isotopes contents analyses, while the second fraction was used to extract zircons using standard separation techniques. The content in major elements (Table 1S in Supplementary material) are as follow: $SiO_2 \approx$ 67-75 wt %, $Na_2O + K_2O \approx$ 7-8 wt %, low contents in MgO ≈ 0.14-0.24 wt %, high $Al_2O_3 \approx$ 14.7-19.7 wt %. Their protoliths are peraluminous granitoids (ASI≈ 1.1.-1.2) (Fig. 5C, D, E and F). In silicate Earth-normalised diagrams they have negative anomalies in Ba, Nb, Sr, Zr, and Ti, and positive anomalies in U, Ta, Pb, and P (Fig. 7; Table 1S in Supplementary material). These rocks have low contents in REE, and also have chondrite-normalised enrichment in LREE relative to

HREE with negative Eu anomalies (Fig. 8; Table 1S in Supplementary material). The rocks also have low values of $^{87}Rb/^{86}Sr$ that are 3.002 and 10.241 with values of $^{87}Sr/^{86}Sr$ of 0.707600 and 0.729318, being $^{87}Sr/^{86}Sr_{335\ Ma}$ of 0.680488 and 0.693285. The values of $^{147}Sm/^{144}Nd$ are 0.166 and 0.169, with $^{143}Nd/^{144}Nd$ values of 0.512401 and 0.512369, being the εNd_{335Ma} of -3-.3 and -4.1 with a $T_{DM(Ga)}$ of 2.0 and 2.2 (see Table 1S in Supplementary material).

Sample AP3-F consists of a leucocratic mylonitised augengneiss. Zircons are abundant and euhedral to subhedral bipyramidal prisms with dimensions about 250 to 100μm (Fig. 8A). Most are brownish translucent crystals. Cathodoluminiscence imaging reveals partial metamictic alteration of several of the small zircons. Well-defined oscillatory zoning can be imaged in most of the grains. U-Pb measurements on 31 different crystals yielded moderate to large concentrations of U (427.0-5869.4ppm) and Th (54.0-489.0ppm) with Th/U = 0.06-0.50 (Table 2S in Supplementary material). The data define a discordia by Pb loss and common Pb with an upper intercept at 271.2 +17.7 -18.8 Ma, and a lower intercept at -13.1 +105.4 -13.1 Ma (MSWD = 2.0913) (Fig. 8B). The 8 data with a higher age and more concordance yield a $^{206}Pb/^{238}U$ Age = 295 ± 4 Ma (mswd= 1.75) (Fig. 8C).

Sample C3F consists of a white mylonitised augengneiss (see Fig. 5B) with centimetric K feldspar porphyroblasts with σ-structures. Zircons are abundant and euhedral to subhedral bipyramidal prisms with dimensions about 250 to 80 μm of major length and 100 to 50 μm width. Most are brownish translucent crystals. Cathodoluminiscence imaging reveals partial metamictic alteration of most of the small zircons and fracture patterns in several crystals; however, well-defined oscillatory zoning can be imaged in several grains (Fig. 8D). U-Pb measurements on 26 different crystals without metamictic alteration yielded moderate to large concentrations of U (349.5-4142.9 ppm) and Th (67.6-902.9

ppm) with Th/U = 0.05-0.62 (Table 3S in Supplementary material). The data define also a discordia by Pb loss and common Pb^{204} (Fig. 8E). The 11 analysis with higher and more concordant ages yield a $^{206}Pb/^{238}U$ Age = 290 ± 5 Ma (mswd= 4.32). All the previous data point to a Sakmarian (early Permian) age for the intrusion of the protoliths of the gneisses.

$^{40}Ar/^{39}Ar$ determinations in micro-populations (2 to 3 grains) of white mica in mylonitized porphyroclasts from the sample AP3-F (Fig. 8F) yield four disturbed spectra with individual total fusion ages between 195.23 ± 0.77 Ma and 205.88 ± 1.52 Ma (Fig. 9, Tables 4S to 7S in Supplementary material) and a weighted mean age of 202.45 ± 0.98 Ma. In one replica, we obtained a mini-plateau age with most of released Argon on one step, corresponding to 47% of ^{39}Ar, of 205.49 ± 1.49 Ma concordant with the total fusion age (205.88 ± 1.52 Ma) (Fig. 9A), and the weighted mean age calculated with all total fusion ages. For all the spectra, the age changes with constant Ca/K, suggesting Ar loss from a homogeneous population (e.g. Negro et al., 2008).

5. Structure

The different tectonic units of the area are separated by a major ductile shear zone roughly striking NE-SW that bounds the upper Tarjât unit from the underlying Taïdant unit. The shear zone is gently dipping towards the NW or NNW. This main ductile shear zone is nicely exposed just below a long section of the road to the lighthouse (Figs. 3 and 4). The main surface is always marked by an iron-bearing carbonate mylonite. The mylonite has a very well defined stretching lineation (L_p, Fig. 10A) with trends varying between N50ºE and N80ºE and small dips gently dipping as undulating towards the NE and the SW. The S-C ductile structures related to the major shear zone document a top-to-the-WSW sense of movement (Fig. 10B).

A S_c crenulation cleavage (Fig. 10D) associated to a NE-SW trending antiform exhibiting a SE-vergence is bending the main fabric of the upper Tarjât unit (Fig. 10D). The reverse limb of the antiform is also cut and duplicated by another ductile shear zone striking N50ºE that dips 30 to 40° towards the NW (Fig. 10C). This shear zone is also underlined by an iron-bearing carbonate mylonite, nicely exposed near the 403 m summit (Fig. 10D and E). The main fabric of the schists is a planar-linear fabric (S_p/L_p) with a schistosity (S_p) and a N50 to N80ºE trending stretching lineation (L_p) (Figs. 10 F and G). Ductile S-C and S-C' structures within the schists and gneisses and asymmetric σ-structures around K feldspar porphyroblasts in the gneisses indicate deformation in a simple shear regime with a SW transport sense.

The lower Taïdant unit exhibits a slaty cleavage with N50ºE strike and dips towards the NW. A pervasive crenulation with an axis trending around N20ºE (Fig. 11) is warping the previous penetrative deformation.

The whole structure of the Tarjât and Taïdant units is tectonically superposed over the more metamorphic Tarjât unit by a major ductile-brittle horizontal fault near the sea level (Figs. 3, 4 and 12A). The main surface is marked downwards by brittle fault rocks: fault gauges and carbonated fault breccias (Figs. 12A and B). The striations measured in the fault zone at the base of the unit have NE-SW trends and subhorizontal dips. Cataclastic structures such as S-C structures and crushed clast trails indicate a SW sense of movement of the hanging wall.

Three major faults bound the horst exhibiting the metamorphic basement of the Cap des Trois Fourches area. It includes the Aït Lahsene Fault, the Râs Izemrân Fault, and the Mersa Taïdant Fault, clockwise (ALF, RIF, and MTF, respectively in Fig. 3).

Towards the northwest, there is the Aït Lahsene Fault, with N50ºE strike and dip of 60° toward the NW (Fig. 3). The Fault exhibits two sets of superimposed striations, one horizontal and a latter one parallel the maximum dip line of the fault. The brittle structures on the fault surface indicate a former left-handed strike-slip sense of movement coeval with of the opening of the Cap des Trois Fourches Tortonian basin, and a younger normal sense of movement imprinting Tortonian pyroclastic layer nearby El Addi (Fig. 3).

To the east, the coast of the peninsula corresponds to the Râs Izemrân Fault that strikes NNE-SSW and has high dips towards the ESE. This normal fault shows a normal regime with a small left-handed oblique component (Fig. 12C).

The Mersa Taïdant Fault (Figs 3, 4, and 12A) is a normal right-handed brittle fault, which extends from the Oued Amekrane to the coast line cutting across all the aforementioned faults (Fig. 3, 4, 12A). This fault has N110ºE strike and dips to the southwest. On the western border of the massif, another normal fault (Oued Amekrâne Fault, OAF in Fig. 3) striking N155ºE bounds the metamorphic basement from the Neogene sediment. This normal fault following the Oued Amekrâne is dipping 80° to the west.

We have measured several small faults along the trace of the Aït Lahsene, Râs Izemrân, and Oued Amekrâne faults (see Figs. 12D to I) that show both normal and reverse slip kinematics. The right-dihedral method (Angelier and Mechler, 1977) allows us reconstructing the palaeostress axes from fault populations. The σ_1, σ_2, and σ_3 axes are trending NNW-SSE, subvertical, and WSW-ENE, respectively. A late open-radius antiform exhibiting an E-W trending axes gently deforms the bedding of the Tortonian rocks together with the basement rock, and probably also the aforementioned faults.

6.-Discussion

The geochemistry of the orthogneisses shows that both major and trace elements have been mobilised during the main metamorphism event that agrees with the later metasomatic event producing kaolinite in the metasediments (see Negro et al., 2007, 2008). However, the data document that the protoliths of the rocks were peraluminous granitoids, and specifically magnesian ones according to Frost et al. (2001) (Fig. 5).

In the silicate Earth-normalised diagrams, they have negative anomalies in Ba, Nb, Sr, Zr, and Ti; and positive anomalies in U, Ta, Pb, and P (Fig. 7), suggesting a crustal-derived signature. These rocks have low contents in REE, and also have chondrite-normalised enrichment in LREE relative to HREE with negative Eu anomalies (Fig. 7). The low values of $^{87}Rb/^{86}Sr$ (3.002 and 10.241) of the orthogneisses suggests that Rb has been mobilized in these rocks agreeing with the previously mentioned metasomatic event, while the $^{147}Sm/^{144}Nd$ (0.166 and 0.169), εNd_{335Ma} (-3.3 and -4.1) and $T_{DM(Ga)}$ (2.0 and 2.2) suggest a significant crustal component that agrees with the crustal-derived signature.

The obtained U-Pb SHRIMP on zircons ages range from 290 to 295 Ma suggesting a Sakmarian (Early Permian) age for the intrusion of the protoliths of the gneisses. Intrusive bodies at the origin of the protoliths are probably related to the Late Variscan magmatic event that is reported throughout the entire Variscan Belt (i.e. Bea, 2004; Casquet and Galindo, 2004; Pereira et al., 2012).

The early Permian age for the igneous protoliths also indicates that the metasedimentary sequence of the upper Tarjât Unit has a Carboniferous or older age. The age of the sequence of the lower Taïdant Unit cannot be determined in the Cap des Trois Fourches area. However, similarities with the early Cretaceous (Aptian-Albian) brown shales and quartzites of the intermediate Temsamane units, together with a similar location below a chloritoid-bearing Paleozoic IP-LT metamorphic unit (Ras Afrou Unit in the Temsamane mountain range and Tarjât unit in the Trois Fourches Peninsula, see Frizon de Lamotte, 1985; Frizon de Lamotte et al., 1991; Azdimousa et al., 2007; Negro et al., 2007, 2008; Jabaloy et al., 2015) suggest an early Cretaceous age for the green and brown shales of the lower Taïdant Unit.

The $^{40}Ar/^{39}Ar$ age analyses of muscovite porphyroclasts from the mylonites (AP3-F sample) are very difficult to interpret due to the disturbed spectra of all the replicates. However, it must be emphasized that the muscovite have retained an uppermost Triassic age at around 202 Ma and have not been re-equilibrated during the later metamorphic events (Negro et al., 2007, 2008; Jabaloy et al., 2015). This uppermost Triassic age from the sample AP3-F could be interpreted as a cooling age following the heat anomaly related to the rifting leading to the opening of the Tethys Ocean. Whatever is the possible origin of the heat event, the most likely interpretation is a partial re-opening of the system in relation with fluids circulation during the mylonitisation processes but at an undetermined age.

Similarities with the Temsamane fold-and-thrust stack include far more than the presence of the chloritoid-bearing Paleozoic IP-LT metamorphic unit. The meso and macrostructures described in this work correlate properly with those previously described in the Temsamane mountain range by Frizon de Lamotte (1985), Frizon de Lamotte et al. (1991), Azdimousa et al. (2007), Booth-Rea et al. (2012) and Jabaloy et al. (2015).

The planar-linear fabric (S_p/L_p) generated in a non-coaxial deformation with a top-to-the-WSW is present in both situations as the main mesostructures and the subsequent SE verging NE-SW trending major folds (F_c) deforming the fabric. Also, in good agreement are: (1) the IP-LT metamorphic conditions recognized in the uppermost metamorphic unit (Negro et al., 2007 and 2008), and (2) the $^{40}Ar/^{39}Ar$ ages indicating that the main metamorphic event took place during the Chattian–Aquitanian times (Negro et al., 2008; Jabaloy et al., 2015).

García-Dueñas et al. (1995) and Sánchez-Gómez (1996) have ascribed the rocks of the Tarjât Unit to the Sebtide/Alpujarride Complex from the Internal Zones of the

Rif/Betic belt. Because the Taïdant Unit is in the uppermost structural situation, they have proposed this unit to be part of the Ghomaride/Malaguide Complex of the Internal Zones. Michard et al. (2007, 2008) have provided the same tectonic interpretation for the Taïdant Unit being in the uppermost position. However, instead of proposing any relationship with the Rif/Betic Internal Zones they correlated the Taïdant Unit with the Ketama Unit and the Tarjât Unit to the highest most metamorphic Temsamane Unit (i.e. the External Zone of the Rif) (Michard et al., 2007, their Fig. 8).

The horizontal brittle-ductile fault at the base of the Taïdant Unit and outcropping at the sea level strongly resembles the fault rocks association, kinematics and geometry of the Temsamane detachment as described by Booth-Rea et al. (2012) and Jabaloy et al. (2015). More precisely, the Cap des Trois Fourches area is similar to the brittle Ait Amrâne klippen and the Khebaba semi-klippe where IP-LT metamorphic rocks are separated by brittle fault rocks from the lowermost Temsamane units (Booth-Rea et al., 2012; Jabaloy et al. 2015). The Tortonian and Messinian sediments and volcanic rocks covering the subhorizontal detachment fault indicate that this fault was exposed at eroding agents during Tortonian times. This is in good agreement with the evolution described in the Boudinar basin further west (Azdimousa et al., 2006; Galindo-Zaldivar et al., 2015; Jabaloy et al., 2015; Achalhi et al., 2016). The last brittle deformation events have recorded a NNW-SSE compression and a WSW-ENE extension of Messinian age. We therefore suggest that the Cap des Trois Fourches Paleozoic rocks are part of the Temsamane fold-and-thrust stack. This interpretation has been previously proposed by Michard et al. (2007, 2008). Also, it was considered that the Paleozoic rocks of the Cap des Trois Fourches extend eastwards into the Kebdana range and western Algeria. As a consequence, we consider that the Paleozoic sediments and igneous rocks of the Cap des Trois Fourches together with the along-trending similar units are remains derived from the

North African palaeomargin involved in the Rif belt. These units were involved as tectonic sheets in the External Zone of the Rif, and originated most probably from the Eastern Moroccan Meseta. They have first recorded the Triassic rifting events and then the collision between the Internal Zones of the Rif belt (i.e. the Alborán domain) and the Tethysian margin of the Africa plate during the Cenozoic times.

As previously mentioned in the geological setting section, the western and eastern Rif exhibit a major contrast in their structural level of tectonic deformation. This is in good agreement with the crustal thickness of both areas that are ~50 km to ~ 24 km, respectively (Mancilla et al., 2012, 2015; Díaz et al., 2016). We infer that the crustal transition step between both domains is located along the active Trougout-Nekor sinistral transtensional system (Asebriy et al., 1993; Barcos et al., 2014; Poujol et al., 2014) at subsurface shallower depth. This transtensional zone system that involves the lithosphere-asthenosphere boundary at depth is considered as accommodating the Present-day movement of the Western Rif towards the WSW with respect to the stable Nubia (see GPS data from Vernant et al., 2010). Thus, forming the southern STEP boundary of the Betic-Rif subduction system. Upward, the active Trougout-Nekor system would be the signature of the crustal step (Fig. 13, location of the cross-section on Fig. 2) at shallower depth. The ductile tectonic deformation identified at the Cap des Trois Fourches together with those recognized in the Temsamane area document a major detachment: the Temsamane detachment system, whose hanging wall moved towards the SW (Azdimousa et al., 2007; Booth-Rea et al., 2012; Jabaloy et al., 2015). To the west, the active Trougout-Nekor fault system (Asebriy et al., 1993; Barcos et al., 2014; Poujol et al., 2014) records a sinistral transtensional movement. This fault system cuts the Temsamane detachment, which is displaced downward by about several km bounding the Ketama unit at depth. At Present time, this detachment is active bounding the western Rif at depth that is moving as a whole, being the hanging wall of the system.

The cross section at Figure 13 agrees with the roll-hinge model (Buck, 1988; Hamilton, 1988; and Wernicke and Axen, 1988; Lavier et al., 1999; Platt et al. 2014) where the Trougout-Nekor fault system is the active section of the detachment whose hanging wall is moving around 4 mm/year^{-1} towards the WSW. The Temsamane detachment represents the inactive section of the detachment as previously proposed by Booth-Rea et al. (2012) and Jabaloy et al. (2015). The strong thinning of the crust along the eastern Rif, which occurred since the Late-Neogene is proposed resulting from the Temsamane detachment fault system at the southern edge of the Betic-Rif subduction system.

7.-Conclusions

We present new lithostratigraphic and geochemical data from the Cap des Trois Fourches area. We describe and date for the first time mylonitised orthogneisses derived from Late Variscan magnesian peraluminous granitoids. Their protoliths were subsequently involved into the Alpine orogeny and associated metamorphism. We also redefine the major metamorphic sequences from the area and we clarify their tectonic relationship. We present a new cartography of the area defining the extension of the Taïdant and Tarjât units and their internal tectonic deformations. A major ductile shear zone separates the Upper Tarjât unit from the Lower Taïdant unit. Tectonic deformation kinematics of the shear zone documents a top-to-the-west sense of movement.

Also, we have identified a major ductile-brittle detachment fault with a top-to-the-west sense of movement. We infer this detachment being an eastward prolongation of the

Temsamane detachment into the des Cap des Trois Fourches area. We provide new U-Pb SHRIMP zircon ages from the orthogneisses indicating a Sakmarian (Early Permian) age for the intrusion of their protoliths. We also determine $^{40}Ar/^{39}Ar$ ages in micro-populations (2 to 3 grains) of white micas from the mylonitised orthogneisses with a weighted mean age of 202.45 ± 0.98 Ma. That age is more probably related to a partial re-opening of the system in relation with fluids circulation during the mylonitisation processes, but at an undetermined age.

We propose a model of the crustal structure of the eastern Rif, where the brittle detachment represents the inactive section from an active detachment responsible for the Present-day movement of the central Rif with respect to the eastern Rif and the different crustal thicknesses between both sectors.

Acknowledgements

We acknowledge the financial support of research grants CGL2015-71692-P and CGL2015-67130- C2-1-R from the Spanish Ministry of Economy and Competitiveness (MINECO/FEDER, Spain). This project has received funds from the FP7-Marie Curie Action IRSES-MEDYNA funded under Grant Agreement PIRSES-GA- 2013-612572. We want to thank Aitor Cambeses for his help with the geochemistry and geochronology of the orthogneisses, and Fernando Nieto for his help with the adquisition and interpretation of the XRD data.

References:

Achalhi, M., Münch, P., Cornée,J.-J. , Azdimousa, A., Melinte-Dobrinescu, M., Quillévéré, F., Drinia, H., Fauquette, S., Jiménez-Moreno, G., Merzeraud, G., Ben Moussa, A., El Kharim, Y., Feddi, N., 2016. The late Miocene Mediterranean-

Atlantic connections through the North Rifian Corridor: New insights from the Boudinar and Arbaa Taourirt basins (northeastern Rif, Morocco). Palaeogeography, Palaeoclimatology, Palaeoecology, 459, 131–152.

Ait Brahim, L., 1991. Tectonique cassante et états de contraintes récents au nord du Maroc; contribution à l'étude du risque sismotectonique. Ph. Doctoral Thesis, University of Rabat, Morocco, 360 p.

Amar, N., Khattach, K., Azdimousa, A., Chourak, M., Jabaloy, A., Ahmed Manar, A., Amar, M., 2015. Structure and peridotite of Gibraltar arc southern bloc: gravimetric and aeromagnetic evidences. Arab. J. Geosci. 8, 11, 9801-9813. doi : 10.1007/s12517-015-1879-3.

Angelier, J., Mechler, P., 1977. Sur une méthode graphique de recherche des contraintes principales également utilisable en tectonique et en séismologie: la méthode des dièdres droits. Bull. Soc. Geol. Fr.7, 6, 1309-1318.

Andrieux, J., 1971. La structure du Rif central. Notes du Service Géologique du Maroc (235 pp., Rabat, Morocco).

Asebriy, L., 1994. Evolution tectonique et métamorphique du Rif central (Maroc): définition du domaine Subrifain. Ph. Doctoral Thesis,, University of Rabat, Morocco, 248 pp.

Asebriy, L., de Luca, P., Bourgois, J., Chotin, P., 1987. Resédimentation d´âge sénonien dans le Rif central (Maroc): conséquences sur les divisions paléogeógraphiques et structurales de la chaîne. J. Afr. Earth Sci. 6, 9–17.

Asebriy, L., Bourgois, J., Cherkaoui, T.E., Azdimousa, A., 1993. Evolution tectonique récente de la zone de faille du Nékor: importance paléogeographique et structurale dans le Rif externe, Maroc. J. African Earth Sci., 17, 65–74.

Asebriy, L., Azdimousa, A., Bourgois, J., 2003. Structure du Rif externe sur la transversale du Massif de Ketama. Trav. Inst. Sci. Rabat, Maroc 21, 27-46.

Azdimousa, A., Bourgois, J., Poupeau, G., Montigny, R., 1998. Histoire thermique du massif de Kétama (Maroc); sa place en Afrique du Nord et dans les Cordillères Bétiques. C. R. Acad. Sci. Paris 326, 847–853.

Azdimousa, A., Bourgois, J., Asebriy, L., Poupeau, G., Montigny, R., 2003. Histoire thermique et surrection du Rif externe et des nappes de flyschs associées (Nord Maroc). Trav. Inst. Sci. Rabat, 21, 15–26.

Azdimousa, A., Poupeau, G., Rezqui, H., Asebriy, L., Bourgois, J., Aït Brahim, L., 2006. Géodynamique des bordures méridionales de la mer d´Alboran; application de la stratigraphie séquentielle dans le bassin néogène de Boudinar (Rif oriental, Maroc). Bull. Inst. Sci. Rabat Sci. Terre, 28, 9-18.

Azdimousa, A., Jabaloy, A., Asebriy, L., Booth-Rea, G., González-Lodeiro, F., Bourgois, J., 2007. Lithostratigraphy and structure of the Temsamane unit (eastern external Rif, Morocco). Rev. Soc. Geol. Esp. 20, 187–200.

Balanyá, J.C., García-Dueñas, V., 1987. Les directions structurales dans le Domaine d'Alborán de part et d'autre du Détroit de Gibraltar. C. R. Acad. Sci., 304, 929–932.

Barcos, L., Jabaloy, A., Azdimousa, A., Asebriy, L., Gómez-Ortiz, D., Rodríguez-Peces, M.J., Tejero, R., Pérez-Peña, J.V., 2014. Study of relief changes related to active doming in the eastern Moroccan Rif (Morocco) using geomorphological indices. J. Afr. Earth Sci., 100, 493–509.

Bea, F., 2004. La naturaleza del magmatismo de la Zona Centro Ibérica: consideraciones generales y ensayo de correlación. In: Vera, J. A. (Ed.), Geología de España. 128-133. Madrid: SGE-IGME.

Ben Yaich, A., 1991. Evolution tectono sédimentaire du Rif externe centro occidental (Régions de Msila et Ouezzane, Maroc). La marge africaine du Jurassique au Crétacé inférieur. Les bassins néogènes d'avant fosse. PhD Thesis, University of Pau, France, 308 p

Benzaggagh, M., Mokhtari, A., Rossi, P., Michard, A., El Maz, A., Chalouan, A., Saddiqi, O., Rjimati, E.-C., 2014. Oceanic units in the core of the External Rif (Morocco): intramargin hiatus or South-Tethyan remnants? J. Geodyn. 77, 4–21. doi: 10.1016/j.jog.2013.10.003.

Bezada, M.J., Humphreys, E.D. Toomey, D.R., Harnafi, M., Davila, J.M., 2013. Evidence for slab rollback in westernmost Mediterranean from improved upper mantle imaging, Earth Planet. Sci. Lett. 368, 51-60.

Booth-Rea, G., Azañón, J.M., Martínez-Martínez, J.M., Vidal, O., García-Dueñas, V., 2005. Contrasting structural and P–T evolutions of tectonic units in the southeastern Betics: key for understanding the exhumation of the Alborán Domain HP/LT crustal rocks (Western Mediterranean). Tectonics 24. doi: 10.1029/2004TC001640.

Booth-Rea, G., Ranero, C.R. Martínez-Martínez, J.M. Grevemeyer, I., 2007. Crustal types and Tertiary tectonic evolution of the Alborán Sea, western Mediterranean. Geochemistry, Geophysics, Geosystems 8 (10), Q10005.

Booth-Rea, G., Jabaloy-Sánchez, A., Azdimousa, A., Asebriy, L., Vázquez-Vílchez, M., Martínez-Martínez, J.M., 2012. Upper-crustal extension during oblique collision: the Temsamane extensional detachment (eastern Rif, Morocco). Terra Nova 24, 505–512. doi: 10.1111/j.1365-3121.2012.01089.x.

Booth-Rea, G., Ranero, C.R., Grevemeyer, I., in press. The Alboran volcanic arc modulated the Messinian faunal exchange and salinity crisis. Scientific Reports in press. Doi:10.1038/s41598-018-31307-7.

Bourgois, J., 1977. D'une étape géodynamique majeure dans la genèse de l´arc de Gibraltar: L´hispanisation des flyschs rifains au Miocène inférieur. Bull. Soc. Geol. Fr. XIX, 115–1119.

Bourgois, J., 1980a. Pre-Triasic fit and alpine tectonics of continental blocks in the western Mediterranean: discussion and reply. Geological Society of America Bulletin, 91, 632-634.

Bourgois, J., 1980b. De l'origine ultra-bétique des Malaguides (zones internes bétiques, Espagne). Geologica Romana, 19, 151-170.

Buck, W. R., 1988. Flexural rotation of normal faults, Tectonics, 7, 959 – 973.

Calvert, A., Sandvol, E., Seber, D., Barazangi, M., Roecker, S., Mourabit, T., Vidal, F., Alguacil, G., Jabour, N., 2000 Geodynamic evolution of the lithosphere and upper mantle beneath the Alboran region of the western Mediterranean: constraints from travel time tomography. J Geophys Res 105, 10871-10898.

Carminati, E., Lustrino, M., Doglioni, C., 2012. Geodynamic evolution of the central and western Mediterranean:.Tectonics vs. igneous petrology constraints. Tectonophysics 579, 173-192

Casquet, C., Galindo, C., 2004. El magmatismo varisco de la Zona de Ossa Morena. In: Geología de España. Vera, J.A. (ed.) SGE-IGME, Madrid, 194-199, ISBN: 84-7840-546-1.

Chalouan, A., Michard, A., 2004. The Alpine Rif belt (Morocco): a case of mountain building in a subduction-subduction-transform fault triple junction. Pure Appl. Geophys. 161 (3), 489–519.

Chalouan, A., Michard, A., El Kadiri, K., Negro, F., Frizon de Lamotte, D., Soto, J.I., Saddiqi, O., 2008. The Rif Belt. In: Michard, A., Frizon de Lamotte, D., Saddiqi, O., Chalouan, A. (Eds.), Continental Evolution: The Geology of Morocco, Lecture

Notes in Earth Sciences. vol. 116. Springer-Verlag, Berlin Heidelberg, pp. 203–302.

Chertova, M.V., Spakman, W., van den Berg, A.P., van Hinsbergen, D.J.J., 2014. Absolute plate motions and regional subduction evolution. Geochemistry, Geophysics, Geosystems 15, 3780-3792, doi: 10.1002/2014GC005494.

Díaz, J., Gil, A., Carbonell, R., Gallart J., Harnafi, M., 2016. Constraining the crustal root geometry beneath Northern Morocco, Tectonophysics. 689, 14-24. doi: 10.1016/j.tecto.2015.12.009.

Duggen, S., Hoernle, K., van den Bogaard, P., Rupke, L., Phipps Morgan, J., 2003. Deep roots of the Messinian salinity crisis. Nature 422, 602-606.

Duggen, S., Hoernle, K., Van den Bogaard, P., Garbe-Schonberg, D., 2005. Post-collisional transition from subduction- to intraplate-type magmatism in the Westernmost Mediterranean: evidence for continental-edge delamination of subcontinental lithosphere. J. Petrol. 46, 1155–1201.

Duggen, S., Hoernle, K., Klugel, A., Geldmacher, J., Thirlwall, M., Hauff, F., Lowry, D., Oates, N., 2008. Geochemical zonation of the Miocene Alboran Basin volcanism (westernmost Mediterranean): geodynamic implications. Contrib Mineral Petr 156, 577-593.

Durand-Delga, M., Hottinger, L., Marcais, J., Mattauer, M., Milliard, Y., Suter, G., 1962. Données actuelles sur la structure du Rif. Livre à la mémoire du professeur Fallot. Soc. Géol. Fr. Mém. 1, 399–442 (Paris).

Duran-Delga, M., Rossi, P., Olivier, P., Puglisi, D., 2000. Situation structurale et nature ophiolitique de roches basiques jurassiques associées aux flyschs maghrébins du Rif (Maroc) et de Sicile (Italie). C. R. Acad. Sci. Paris II 331 (1), 29–38.

Faccenna, C., Piromallo, C., Crespo-Blanc, A., Jolivet, L., Rossetti, F., 2004. Lateral slab deformation and the origin of the western Mediterranean arcs. Tectonics 23. Doi: 10.1029/2002TC001488.

Favre, P., 1992. Géologie des massifs calcaires situés au front Sud de l'unité de Kétama (Rif, Maroc). PhD Thesis. University of Genève.

Feinberg, H., 1986. Les séries tertiaires du Prérif et des dépendances post tectoniques du Rif (Maroc). PhD Thesis, University of Toulouse.

Fernandez Navarro, L., 1911. Estudios geológicos del Rif oriental. Memorias de Real Sociedad Española de Historia Natural. Tome XIII

Frizon de Lamotte, D., 1985. La structure du Rif oriental (Maroc). Rôle de la tectonique longitudinale et importance des fluides. Ph.D. Thesis, University Paul et Marie Curie, Paris VI, France (436 pp.).

Frizon de Lamotte, D., 1987. Un exemple de collage synmétamorphe: la déformation miocène des Temsamane (Rif externe, Maroc). Bull. Soc. Geol. Fr. 3, 337–344.

Frizon de Lamotte, D., Andrieux, J., Guezou, J.-C., 1991. Cinématique des chevauchements néogènes dans l'Arc bético-rifain: discussion sur les modèles géodynamiques, Bull. Soc. Géol. Fr., 169, 611-626.

Frost, B.R., Arculus, R.J., Barnes, C.G, Collins, W.J, Ellis, D.J, Frost, C.D., 2001. A geochemical classification of granitic rocks. Journal of Petrology, 42, 2033-2048.

Galindo-Zaldívar, J., Azzouz, O., Chalouan, A., Pedrera, A., Ruano, P., Ruiz-Constán, A., Sanz de Galdeano, C., Carlos Marín-Lechado, C., López-Garrido, A-C., Anahnah, A., Benmakhlouf, M., 2015. Extensional tectonics, graben development and fault terminations in the eastern Rif (Bokoya– Ras Afraou area). Tectonophysics, 663, 140- 149. doi: 10.1016/j.tecto.2015.08.029

García-Dueñas, V., Balanyá, J.C., Sánchez-Gómez, M., 1995. El Despegue extensional de Lahsene y los jirones de serpentinitas del anticlinal de Taryat (Melilla, Rif). Geogaceta, 17, 138–139.

Govers, R., Wortel, M.J.R., 2005. Lithosphere tearing at STEP faults: response to edges of subduction zones. Earth Planet Sc Lett 236, 505-523.

Guillemin, M., Hernandez, J., Wildi, W., 1983. Carte géologique du Rif, échelle 1/50 000, feuille Melilla. Notes et Mémoires du Service géologique du Maroc, 297.

Guillemin, M., Houzay, J. P., 1982. Le Néogène post-nappes et le Quaternaire du Rif Nord oriental. Stratigraphie et tectonique des bassins de Melilla, de Kert, de Boudinar et du piémont des Kebdana. Notes et Mémoires du Service Géologique du Maroc, 314, 7–239.

Hamilton, W.B., 1988. Detachment faulting in the Death Valley region, California and Nevada: U.S. Geological Survey Bulletin, 1790, 51–85.

Hermann, J., Müntener, O., Scambelluri, M., 2000. The importance of serpentinite mylonites for subduction and exhumation of oceanic crust. Tectonophysics, 327, 225-238.

Hernández, J., Bellón, H., 1985. Chronologie K-Ar du volcanisme miocène du Rif oriental (Maroc): implications tectoniques et magmatologiques. Revue de Géologie Dynamique et de Géographie Physique, 26, 85-94.

Jabaloy-Sanchez, A., Azdimousa, A., Booth-Rea, G., Asebriy, L., Vazquez-Vilchez, M., Miguel Martinez-Martinez, J., Gabites, J., 2015. The structure of the Temsamane fold-and-thrust stack (eastern Rif, Morocco): Evolution of a transpressional orogenic wedge. Tectonophysics, 663, 150-176. Doi: 10.1016/j.tecto.2015.02.003.

Jolivet, L., Faccenna, C., Goffé, B., Burov, E., Agard, P., 2003. Subduction tectonics and exhumation of high-pressuremetamorphic rocks in the Mediterranean orogens. Am. J. Sci., 303, 353–409.

Kerzazi K., 1994. Etudes biostratigraphique du Miocène sur la base des foraminifères planctoniques et nannofossiles calcaires dans le Prérif et la marge atlantique du Maroc (site 547A du DSDP Leg 79); aperçu sur leur paléoenvironnement. PhD Thesis, University Pierre et Marie Curie, Paris, 230 pp.

Lavier, L.L., Buck, W.R., Poliakov, A.N.B., 1999, Self-consistent rolling-hinge model for the evolution of large-offset low-angle normal faults: Geology, 27, 1127–1130.

Leblanc, D., 1975–1979. Etude géologique du Rif externe oriental au Nord de Taza (Maroc). Notes et Mémoires du Service Géologique du Maroc, 281 p.

Le Maitre, R.W., 1989. A Classification of Igneous Rocks and Glossary of Terms. Recommendations of the IUGS Commission on the Systematics of Igneous Rocks. Oxford, Blackwell, 256 pp.

Levy, R.G., Tilloy, R., 1952. Maroc septentrional (chaîne du Rif). Partie B, livret guide des excursions A31.C31. In : Congrès Géologique International, XIX session- Alger, série : Maroc, pp 8-65.

Mancilla, F. L., Stich, D., Morales, J., Julià, J., Diaz, J., Pazos, A., Córdoba, D., Pulgar, J.A., Ibarra, P., Harnafi, M., Gonzalez-Lodeiro, F., 2012. Crustal thickness variations in northern Morocco. J. Geophys. Res., 117, B02312. doi: 10.1029/2011JB008608.

Mancilla, F.L., Booth-Rea, G., Stich, D., Pérez-Peña, J. V., Moreles, J., Azañón, J. M., Martin, R., Flavio Giaconia, F., 2015. Slab rupture and delamination under the

Betics and Rif constrained from receiver functions. Tectonophysics, 663, 225–237. doi : 10.1016/j.tecto.2015.06.028

Mancilla, F.L., Diaz, J., 2015. High resolution Moho topography map beneath Iberia and Northern Morocco from receiver function analysis. Tectonophysics, 203–211, doi: 10.1016/j.tecto.2015.06.017.

Martínez-Martínez, J.M., Booth-Rea, G., Azañón, J.M., Torcal, F., 2006. Active transfer fault zone linking a segmented extensional system (Betics, southern Spain): Insight into heterogeneous extension driven by edge delamination. Tectonophysics 422, 159-173.

McDonough, W.F., Sun, S.S., 1995. The composition of the Earth. Chemical Geology, 120, 223-253.

Michard, A., 1976. Elements de Géologie Marocaine. Notes Mémoires du Service Géologique du Maroc 258, 408.

Michard, A., Feinberg, H., El-Azzab, D., Bouybaouène, M., Saddiqi, O., 1992. A Serpentinite ridge in a collisional paleomargin setting: the Beni Malek Massif, external Rif, Morocco. Earth Planet. Sci. Lett. 113 (3), 425–442.

Michard, A., Frizon de Lamotte, D., Negro, F., Saddiqi, O., 2007. Serpentinite slivers and metamorphism in the External Maghrebides: arguments for an intracontinental suture in the African paleomargin (Morocco, Algeria). Rev. Soc. Geol. Esp. 20, 173–185.

Michard, A., Hoepffner, A., Soulaimana, A., Baidder, L., 2008. The Variscan Belt. In Michard, A.; Saddiqi, O.; Chalouan, A.; Frizon de Lamotte, D., eds. Continental evolution: the geology of Morocco. Berlin, Springer, 133–202.

Monié, P., Frizon de Lamotte, D., Leikine, M., 1984. Etude géochronologique préliminaire par la méthode 39Ar/ 40Ar du métamorphisme alpin dans le Rif externe (Maroc).

Précisions sur le calendrier tectonique tertiaire. Revue du Géologie Dynamique et du Géographie physique, 25, 307-317.

Morel, J.L. (1988) Evolution récente de l'orogène rifain et de son avant-pays depuis la fin de la mise en place des nappes (Rif, Maroc). Geodiffusion Mémoires, University Paris-Sud, 4, 583 pp.

Münch, P., Roger, S., Cornee, J.-J., Saint Martin, J.-P., Feraud, G., Benmoussa, A., 2001. Restriction des communications entre l'Atlantique et la Méditerranée au Messinien : apport de la téphrochronologie dans la plate-forme carbonatée et le bassin de Melilla–Nador (Rif nord-oriental, Maroc). C. R. Acad. Sci. 332, 9, 569–576.

Münch, P., Cornee, J.-J., Feraud, G., Saint Martin, J.-P., Ferrandini, M., Garcia, F., Conesa, G., Moullade, M., Roger, S., 2006. Precise $^{40}Ar/^{39}Ar$ chronostratigraphy of the upper Messinian Melilla carbonate complex (NE Morocco): implications for the Messinian Salinity Crisis. International Journal of Earth Sciences, 95, 491–503.

Negro, F., 2005. Exhumation des roches métamorphiques du domaine d´Alboran: étude de la Chaine Rifaine (Maroc) et corrélation avec les Cordillères Bétiques (Espagne). Ph.D. Thesis, University of Paris XI.

Negro, F., Agard, P., Goffé, B., Saddiqi, O., 2007. Tectonic andmetamorphic evolution of the Temsamane units, External Rif (northern Morocco): implications for the evolution of the Rif and the Betic–Rif arc. J. Geol. Soc. Lond. 164, 829–842.

Negro, F., de Sigoyer, J., Goffé, B., Saddiqi, O., Villa, I.M., 2008. Tectonic evolution of the Betic–Rif arc: new constraints from $^{40}Ar/^{39}Ar$ dating on white micas in the Temsamane units (External Rif, northern Morocco). Lithos, 106, 93–108. doi : 10.1016/j.lithos.2008.06.011.

Palomeras, I., Thurner, S., Levander, A., Liu, K., Villaseñor, A., Carbonell, R., Harnafi, M., 2014. Finite-frequency Rayleigh wave tomography of the western

Mediterranean: Mapping its lithospheric structure. Geochemistry, Geophysics, Geosystems 15, 140-160, doi:10.1002/2013GC004861.

Pereira, M.F., Chichorro, M., Silva, J.B., Ordóñez-Casado, B., Lee, J.K.W., Williams, I.S., 2012. Early Carboniferous wrenching, exhumation of high-grade metamorphic rocks and basin instability in SW Iberia: constraints derived from structural geology and U–Pb and 40Ar–39Ar geochronology. Tectonophysics, 558–559, 28–44.

Pereira, M.F., Solá, A. R., Chichorro, M., Lopes, L., Gerdes, A., Silva, J.B., 2012. North-Gondwana assembly, break-up and paleogeography: U-Pb isotope evidence from detrital and igneous zircons of Ediacaran and Cambrian rocks of SW Iberia. Gondwana Res., 22, 866–881.

Pérouse, E., Vernant, P., Chery, J., Reilinger, R., McClusky, S., 2010. Active surface deformation and sublithospheric processes in the western Mediterranean constrained by numerical models. Geology 38(9), 823-826, doi:10.1130/G30963.1.

Platt, J.P., Soto, J.I., Whitehouse, M.J., Hurford, A.J., Kelley, S.P., 1998. Thermal evolution, rate of exhumation, and tectonic significance of metamorphic rocks from the floor of the Alboran extensional basin, western Mediterranean. Tectonics 17, 671-689.

Platt, J.P., Behr, W.M., Johanesen, K., Williams, J.R., 2013. The Betic–Rif arc and its orogenic hinterland: a review. Ann. Rev. Earth Planet. Sci., 41, 14.1–14.45. doi: 10. 1146/annurev-earth-050212-123951.

Platt, J. D., Rudnicki, J.W. Rice, J. R., 2014. Stability and localization of rapid shear in fluid-saturated fault gouge: 2. Localized zone width and strength evolution, J. Geophys. Res. Solid Earth, 119, 4334–4359, doi: 10.1002/2013JB010711.

Poujol, A., Ritz, J.-F., Tahayt, A., Vernant, P., Condomines, M., Blard, P.-H., Billant, J., Vacher, L., Tibari, B., Hni, L., Koulali, A., 2014. Active tectonics of the Northern

Rif (Morocco) from Geomorphic and Geochronological Data. J.Geodyn., 77, 70–88.

Roger, S., Münch, P., Cornée, J.J., Saint Martin, J.P., Féraud, G., Pestrea, S., Conesa, A., Benmoussa, A., 2000. $^{40}Ar/^{39}Ar$ dating of the pre-evaporitic Messinian marine sequences of the Melilla basin (Morocco): a proposal for some biosedimentary events as isochrons around the Alboran Sea. Earth and Planetary Science Letters, 179, 101-113.

Rosenbaum, G., Lister, G.S., Duboz, C., 2002. Reconstruction of the tectonic evolution of the western Mediterranean since the Oligocene. J. Virtual Explor. 8, 107-130.

Sánchez-Gómez, M., 1996. Emplazamiento intracortical y desmembramiento extensional de los cuerpos peridotíticos de Ronda y del Rif (Arco de Gibraltar). Ph.D. Thesis, University of Granada. Spain.

Seber, D., Barazangi, M., Ibenbrahim, A., Demnati, A., 1996. Geophysical evidence for lithospheric delamination beneath the Alboran Sea and Rif-Betic mountains. Nature 379, 785-790.

Shand, S.J., 1947. Eruptive Rocks. Their Genesis, Composition, Classification, and Their Relation to Ore-Deposits with a Chapter on Meteorite. New York, John Wiley & Sons, 360 pp.

Suter, G., 1980a. Carte géologique du Rif, 1/500.000, Map 245a, Geol. Surv. of Morocco, Rabat.

Suter, G., 1980b. Carte structurale du Rif, 1/500.000, Map 245b, Geol. Surv. of Morocco, Rabat.

Thurner, S., Palomeras, I., Levander, A., Carbonell, R., 2014. Evidence for Ongoing Lithospheric Removal in the Western Mediterranean: Ps Receiver Functions

Results From the PICASSO Project. Geochemistry, Geophysics, Geosystems 15, 1113-1127, doi:10.1002/2013GC005124.

van Assen, E., Kuiper, K.F., Barhoun, N., Krijgsman, W., Sierro, F.J., 2006, Messinian astro chronology of the Melilla Basin: Stepwise restriction of the Mediterranean-Atlantic connection through Morocco: Palaeogeography, Palaeoclimatology, Palaeoecology, 238,15–31, doi: 10.1016/j.palaeo.2006.03.014.

Varas-Reus, M.I., Garrido, C.J., Marchesi, C., Bosch, D., Acosta-Vigil, A., Hidas, K., Barich, A., Booth-Rea, G., 2017. Sr-Nd-Pb isotopic systematics of crustal rocks from the western Betics (S. Spain): Implications for crustal recycling in the lithospheric mantle beneath the westernmost Mediterranean. Lithos, 276, 45-61.

Vázquez, M., Asebriy, L., Azdimousa, A., Jabaloy, A., Booth-Rea, G., Barbero, L., Mellini, M., González-Lodeiro, F., 2013. Evidence of extensionalmetamorphismassociated to Cretaceous rifting of the North-Maghrebian passive margin: the Tanger–Ketama unit (External Rif, northern Morocco). Geol. Acta 11, 277–293.

Vernant, P., Fadil, A., Mourabit, T., Ouazar, D., Koulali, A., Davila, J. M., Garate, J., Mc Clusky,S., . Reilinger, R. E., 2010. Geodetic constraints on active tectonics of the Western Mediterranean: Implications for the kinematics and dynamics of the Nubia-Eurasia plate boundary zone, J. Geodyn., 49, 123–129, doi:10.1016/j.jog.2009.10.007.

Vidal, J.F., 1971. Une interprétation nouvelle des nappes du Prérif central (Maroc) et ses conséquences sur la structure de leur substratum autochtone. C. R. Acad. Sci., Paris, D 272, 24–27.

Villaseñor, A., Chevrot, S., Harnafi, M., Gallart, J., Pazos, A., Serrano, I., Córdoba, D., Pulgar, J.A., Ibarra, P., 2015. Subduction and volcanism in the Iberia–North Africa collision zone from tomographic images of the upper mantle. Tectonophysics 663, 238-249.

Wernicke, B. and Axen, G.J., 1988. On the role of isostasy in the evolution of normal fault systems, Geology 16, 848-851.

Figure captions:

Figure 1.- Geological map of the northwestern Africa, including the velocity data of the GPS sites with respect to stable Nubia (Vernant et al., 2010). The location of the study area (Fig.2) is shown.

Figure 2.- A) Main geological domains of the Betic-Rif orogenic system surrounding the Alborán Sea. B) Geological map of the Eastern Rif area with the kinematic vectors from the ductile shear zones and the brittle faults (modified from Jabaloy et al., 2015). Velocity data of the GPS sites with respect to stable Nubia in red (Vernant et al., 2010). Location of Fig. 3 is shown. 1-1' shows the location of the Fig. 13 profile.

Figure 3.- Geological map of the Cap des Trois Fourches area. See Figure 2 for location. Red stars show the location of the orthogneisses samples. Yellow star marks the location of the chloritite sample. Main brittle faults: ALF–Aït Lahsene Fault, DBDF-Ductile-Britlle Detachment fault, MTF–Mersa Taïdant Fault, OAF–Oued Amekrâne Fault, RIF– Râs Izemrân Fault,. Location of Fig.4 cross-sections is shown.

Figure 4.- Geological cross-sections of the Cap des Trois Fourches area. See Fig. 3 for location. Key of Color is same as on Fig. 3.

Figure 5.-

A) Panoramic view (looking to the west) of the orthogneisses lens-shaped bodies within the grey chloritoid-bearing micaschists (the white bed at the upper left is 20 to 25 cm thick). B) Hand specimen of the orthogneis sample C3F, note the abundance of K feldspar porphyroblasts with σ-structures. See Fig. 3 for sample location. C to F) Orthogneisses whole-rock compositions: C) Total alkalis *vs* SiO_2 (TAS) (fields from Le Maitre, 1989). D) Molar $Al_2O_3/(Na_2O+K_2O)$ *vs* Molar $Al_2O_3/(CaO+ Na_2O+K_2O)$ (fields from Shand, 1947). E) Modified alkali-lime index diagram MALI = $Na_2O + K_2O - CaO$ *vs* SiO_2 (Frost et al., 2001). F) Molar (FeOT +MgO)/(MgO) *vs* SiO_2 (Frost et al. 2001). Th–Tholeiitic; Ca–Calc-alkaline; Alk–Alkaline.

Figure 6.- X-ray powder diffractogram of the chloritite sample CTF2. See Figure 3 for location.

Figure 7.- Silicate Earth- and chondrite-normalized diagrams of the orthogneisses (normalization values from McDonough and Sun (1995).

Figure 8.- A) Cathodoluminescence images of representative analyzed zircons of sample AP3-F. See Figure 3 for location. B) Wetherill concordia plot for the whole analyzed zircons from the sample AP3-F. C) Wetherill concordia plot for the analyzed zircons from the sample AP3-F with a higher age and more concordance. D) Cathodoluminescence images of representative analyzed zircons of sample C3F. See Figure 3 for location. E) Wetherill concordia plot for the whole analyzed zircons from the sample C3F. F) View of white mica mylonitized porphyroclasts from the sample AP3-F, similar to those used in $^{40}Ar/^{39}Ar$ determinations.

Figure 9.- Diagrams of cumulative ^{39}Ar Percent v. Age (Ma) of white mica mylonitized porphyroclasts

from the sample AP3-F. To the left, the replica with a mini-plateau age corresponding to 47% of ^{39}Ar, of 205.49 ± 1.49 Ma, concordant with the total fusion age (205.88 ± 1.52 Ma). To the right, the three replicas without plateau ages (see text for discussion). In every graphic, the box heights are 2σ.

Figure 10.- Mesoestructures from the Tarjât unit: A) upper view of the S_p foliation and L_p stretching lineation within grey chloritoid-bearing micaschists. B) Ductile S-C structure in the grey micaschists. C) Incipient S_c crenulation cleavage deforming the grey micaschists. D) mylonitic yellow marbles exhibiting asymmetric boudins of dolomitic marbles. E) View of the ductile shear zone duplicating the Tarjât unit, east of Oued Amekrâne. F and G) Diagrams representing the orientation of ductile mesostructures: F: L_p stretching lineation, and G) F_p axes of microfolds. For all the diagrams: Wulff steronet, lower hemisphere.

Figure 11.- Mesoestructures from the Taïdant unit: A) view of the main foliation of the green and brown shales deformed by microfolds, and B) Diagram representing the orientation of the intersection lineation and microfold axis deforming the main foliation of the shales. For the diagram: Wulff steronet, lower hemisphere.

Figure 12.- A and B) View of the horizontal brittle-ductile fault and fault gouges outcropping at the coast that superposes out-of-sequence the Taïdant unit over the Tarjât one. C) View of the Râs Izemrân Fault zone. D and E) Diagram with the orientation of small faults along the trace of the Aït Lahsene Fault (D) and the result of the right-dihedral method (Angelier and Mechler, 1977) of the same fault population (E). F and G) Diagram with the orientation of small faults along the trace of the Râs Izemrân Fault (F) and the result of the right-dihedral method (Angelier and Mechler, 1977) of the same fault population (G). H and I) Diagram with the orientation of small faults along the trace of the Oued Amekrâne Fault (H) and the result of the right-dihedral method (Angelier and Mechler, 1977) of

the same fault population (I). For all the diagrams: Wulff steronet, lower hemisphere.

Figure 13.- A) Crustal model of the eastern Rif and the transition towards the central Rif area. The Moho depths are from Mancilla et al. (2012, 2015) and Díaz et al. (2015), while the velocity data of the GPS sites with respect to Nubia stable are from Vernant et al. (2010). B) Possible crustal model of the eastern Rif before the movement of the Temsamane detachment fault during Late Miocene to Present-day times.

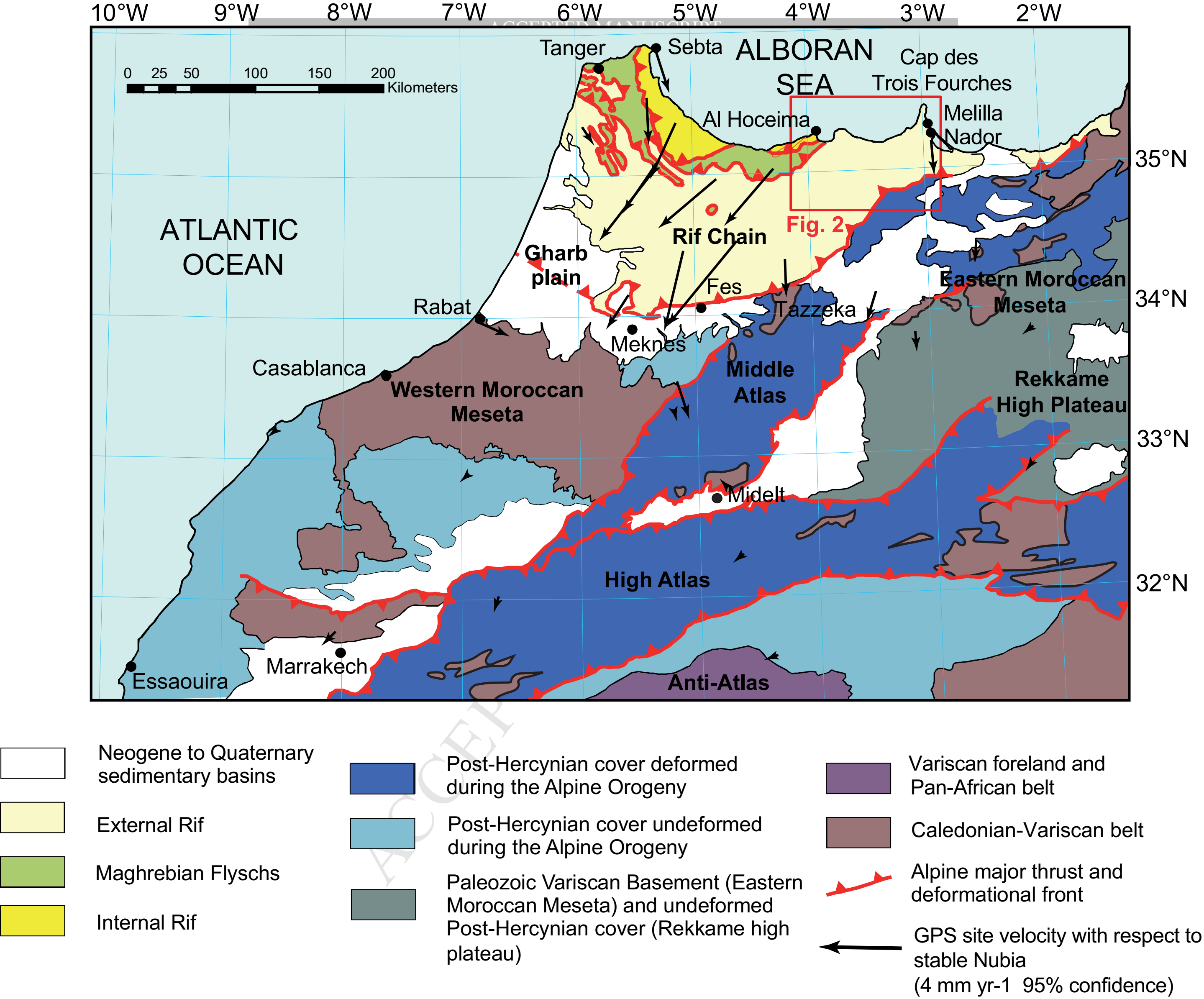
10°W
9°W
8°W
7°W
6°W
5°W
4°W
3°W
2°W
35°N
34°N
33°N
32°N
0 25 50 100 150 200
Kilometers
Tanger
Sebta
ALBORAN SEA
Cap des Trois Fourches
Al Hoceima
Melilla
Nador
Fig. 2
ATLANTIC OCEAN
Gharb plain
Rif Chain
Fes
Tazzeka
Eastern Moroccan Meseta
Rabat
Meknes
Casablanca
Western Moroccan Meseta
Middle Atlas
Rekkame High Plateau
Midelt
High Atlas
Marrakech
Essaouira
Anti-Atlas
Neogene to Quaternary sedimentary basins
External Rif
Maghrebian Flyschs
Internal Rif
Post-Hercynian cover deformed during the Alpine Orogeny
Post-Hercynian cover undeformed during the Alpine Orogeny
Paleozoic Variscan Basement (Eastern Moroccan Meseta) and undeformed Post-Hercynian cover (Rekkame high plateau)
Variscan foreland and Pan-African belt
Caledonian-Variscan belt
Alpine major thrust and deformational front
GPS site velocity with respect to stable Nubia
(4 mm yr-1 95% confidence)

Figure 1

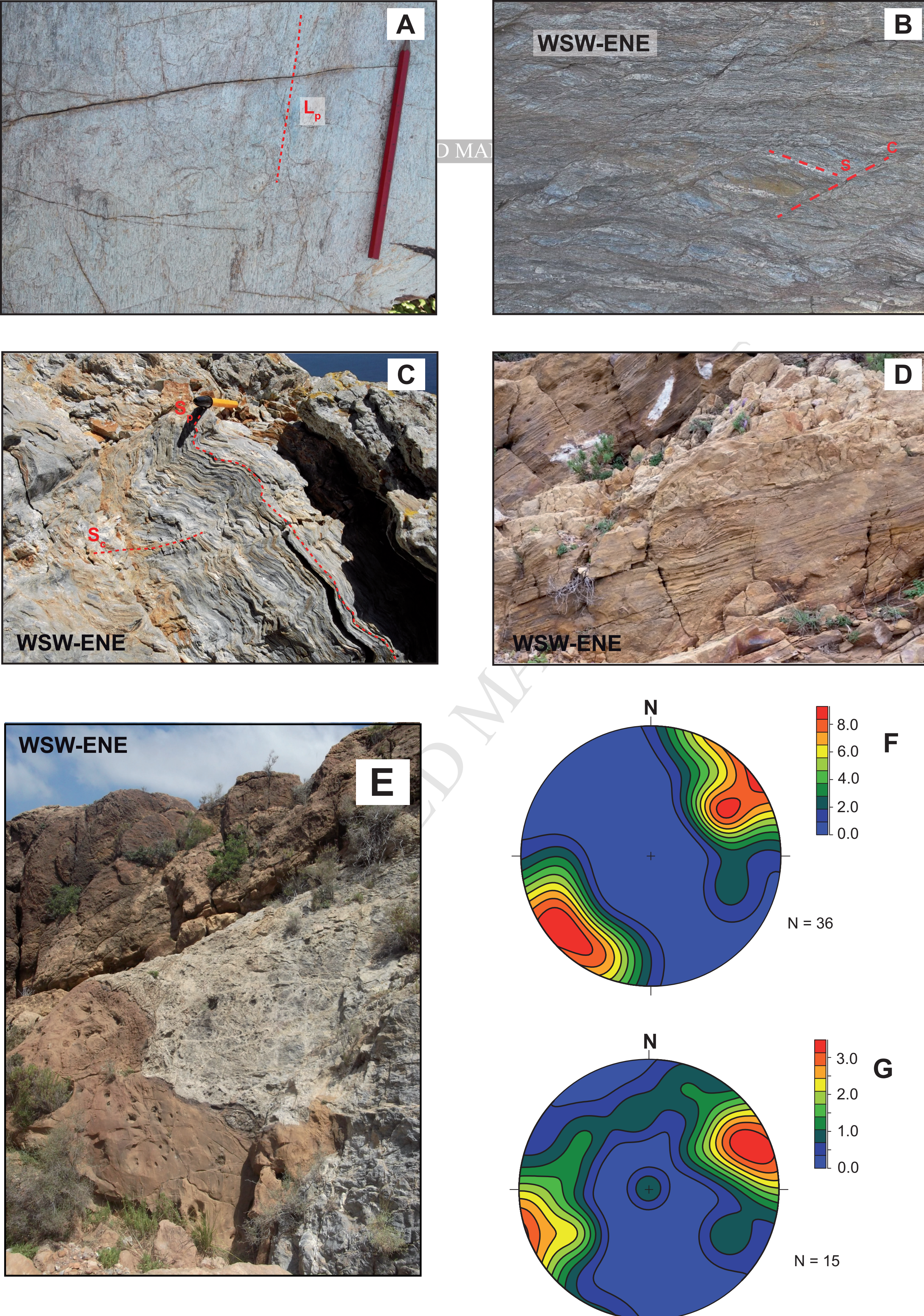
A
L_p
B
WSW-ENE
S
C
C
S_p
S_c
WSW-ENE
D
WSW-ENE
E
WSW-ENE
N
8.0
6.0
4.0
2.0
0.0
F
N = 36
N
3.0
2.0
1.0
0.0
G
N = 15

Figure 10

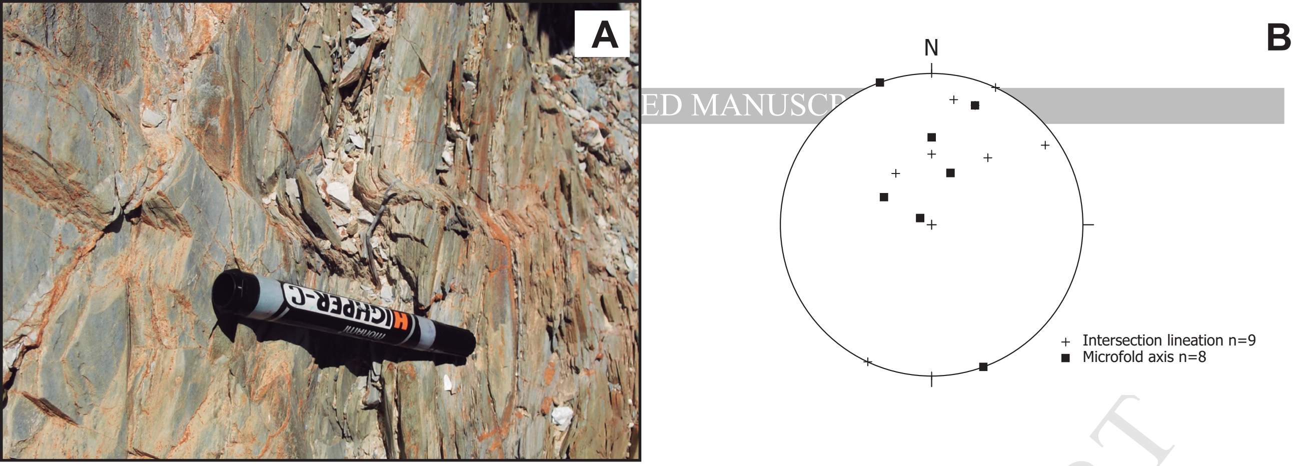

Figure 11

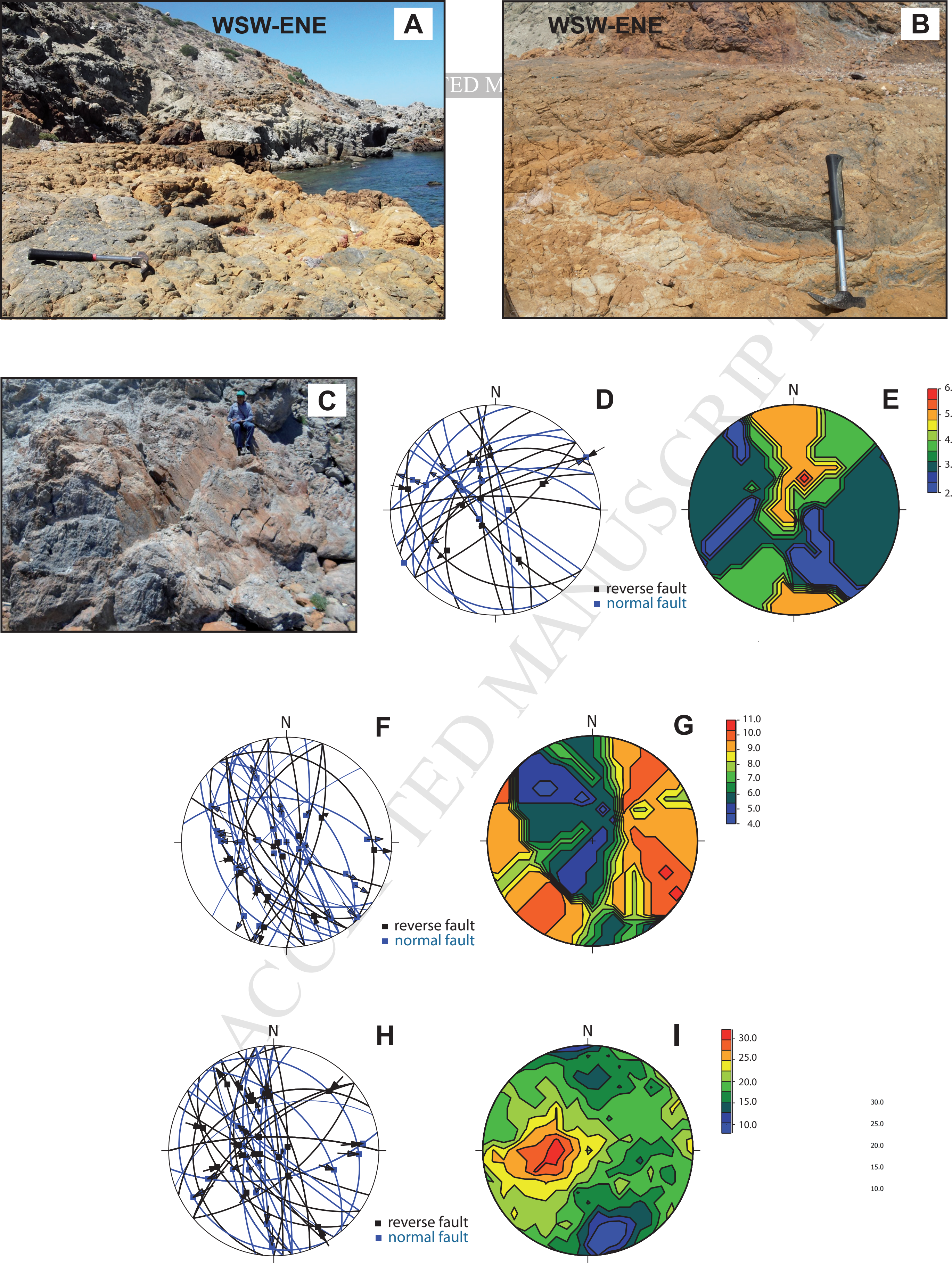

WSW-ENE
A
WSW-ENE
B
C
N
D
reverse fault
normal fault
N
E
6.0
5.0
4.0
3.0
2.0
N
F
reverse fault
normal fault
N
G
11.0
10.0
9.0
8.0
7.0
6.0
5.0
4.0
N
H
reverse fault
normal fault
N
I
30.0
25.0
20.0
15.0
10.0
30.0
25.0
20.0
15.0
10.0

Figure 12

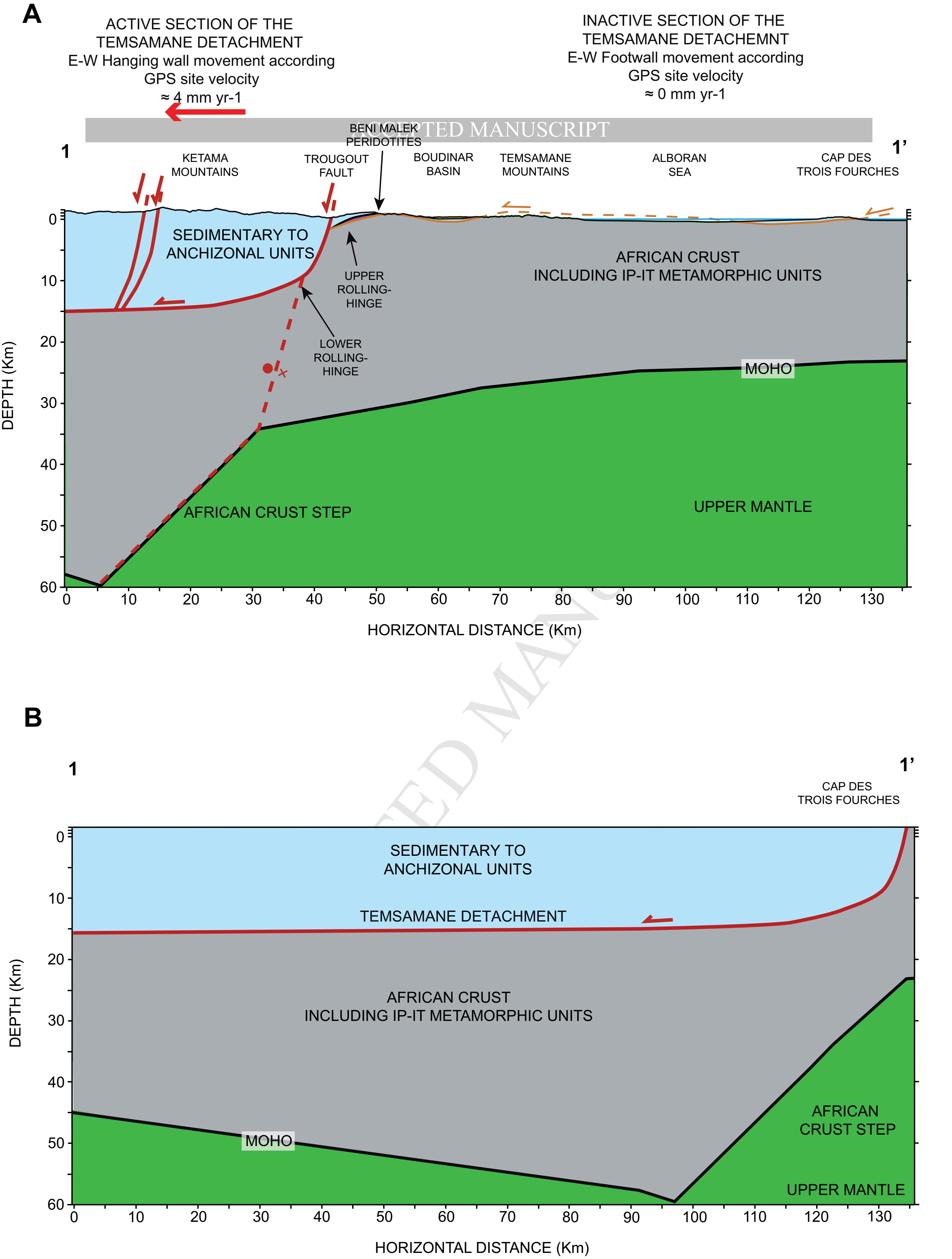
A
ACTIVE SECTION OF THE
TEMSAMANE DETACHMENT
E-W Hanging wall movement according
GPS site velocity
≈ 4 mm yr-1
INACTIVE SECTION OF THE
TEMSAMANE DETACHEMNT
E-W Footwall movement according
GPS site velocity
≈ 0 mm yr-1
1
1'
KETAMA
MOUNTAINS
TROUGOUT
FAULT
BENI MALEK
PERIDOTITES
BOUDINAR
BASIN
TEMSAMANE
MOUNTAINS
ALBORAN
SEA
CAP DES
TROIS FOURCHES
SEDIMENTARY TO
ANCHIZONAL UNITS
UPPER
ROLLING-
HINGE
LOWER
ROLLING-
HINGE
AFRICAN CRUST
INCLUDING IP-IT METAMORPHIC UNITS
MOHO
AFRICAN CRUST STEP
UPPER MANTLE
DEPTH (Km)
HORIZONTAL DISTANCE (Km)
B
1
1'
CAP DES
TROIS FOURCHES
SEDIMENTARY TO
ANCHIZONAL UNITS
TEMSAMANE DETACHMENT
AFRICAN CRUST
INCLUDING IP-IT METAMORPHIC UNITS
MOHO
AFRICAN
CRUST STEP
UPPER MANTLE
DEPTH (Km)
HORIZONTAL DISTANCE (Km)

Figure 13

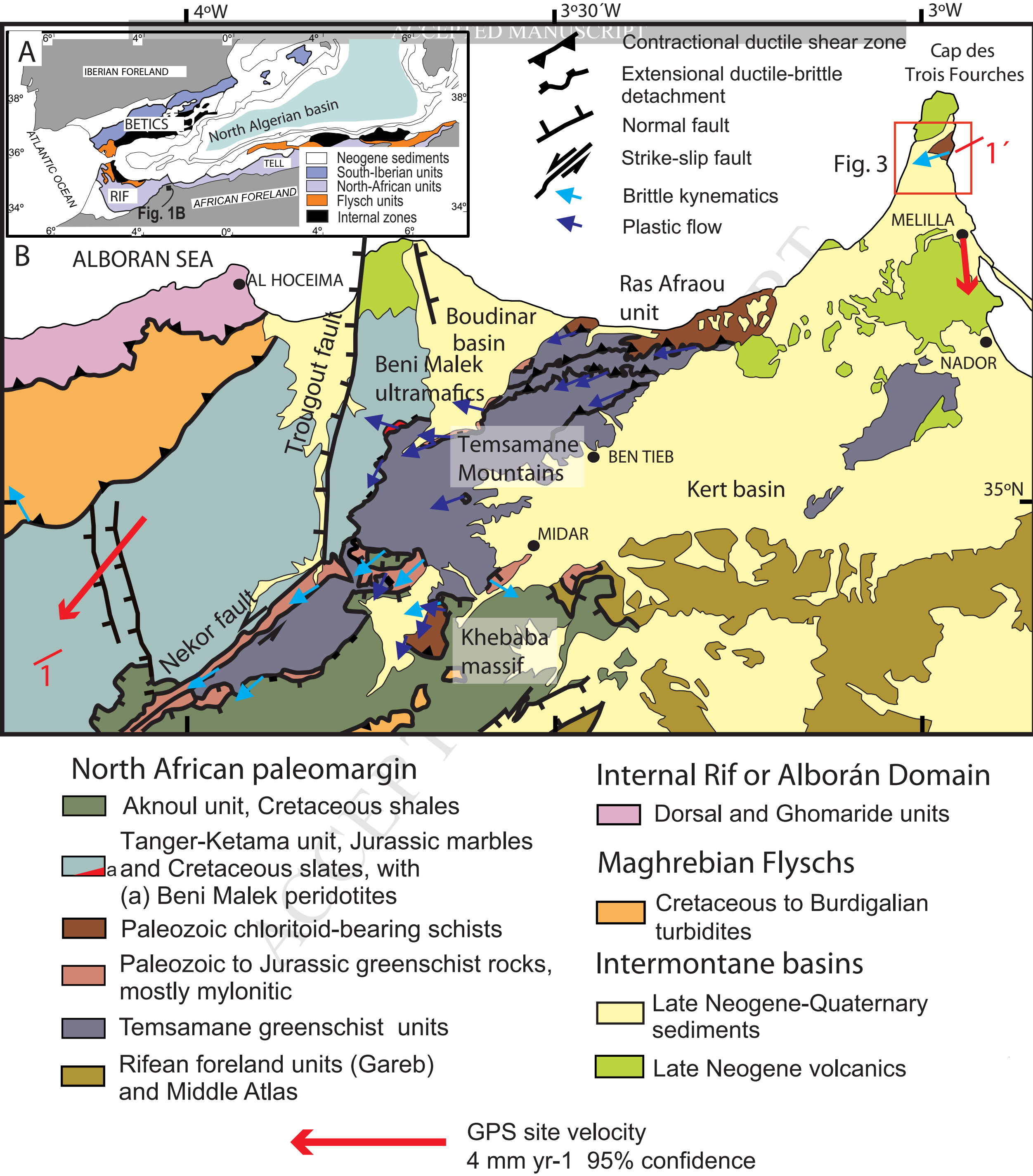

4°W
3°30´W
3°W
A
IBERIAN FORELAND
BETICS
North Algerian basin
ATLANTIC OCEAN
TELL
RIF
AFRICAN FORELAND
Fig. 1B
Neogene sediments
South-Iberian units
North-African units
Flysch units
Internal zones
Contractional ductile shear zone
Extensional ductile-brittle detachment
Normal fault
Strike-slip fault
Brittle kynematics
Plastic flow
Cap des Trois Fourches
Fig. 3
1´
MELILLA
B
ALBORAN SEA
AL HOCEIMA
Trougout fault
Boudinar basin
Beni Malek ultramafics
Ras Afraou unit
NADOR
Temsamane Mountains
BEN TIEB
Kert basin
35°N
MIDAR
Nekor fault
Khebaba massif
1
North African paleomargin
Aknoul unit, Cretaceous shales
Tanger-Ketama unit, Jurassic marbles and Cretaceous slates, with (a) Beni Malek peridotites
a
Paleozoic chloritoid-bearing schists
Paleozoic to Jurassic greenschist rocks, mostly mylonitic
Temsamane greenschist units
Rifean foreland units (Gareb) and Middle Atlas
Internal Rif or Alborán Domain
Dorsal and Ghomaride units
Maghrebian Flyschs
Cretaceous to Burdigalian turbidites
Intermontane basins
Late Neogene-Quaternary sediments
Late Neogene volcanics
GPS site velocity
4 mm yr-1 95% confidence

Figure 2

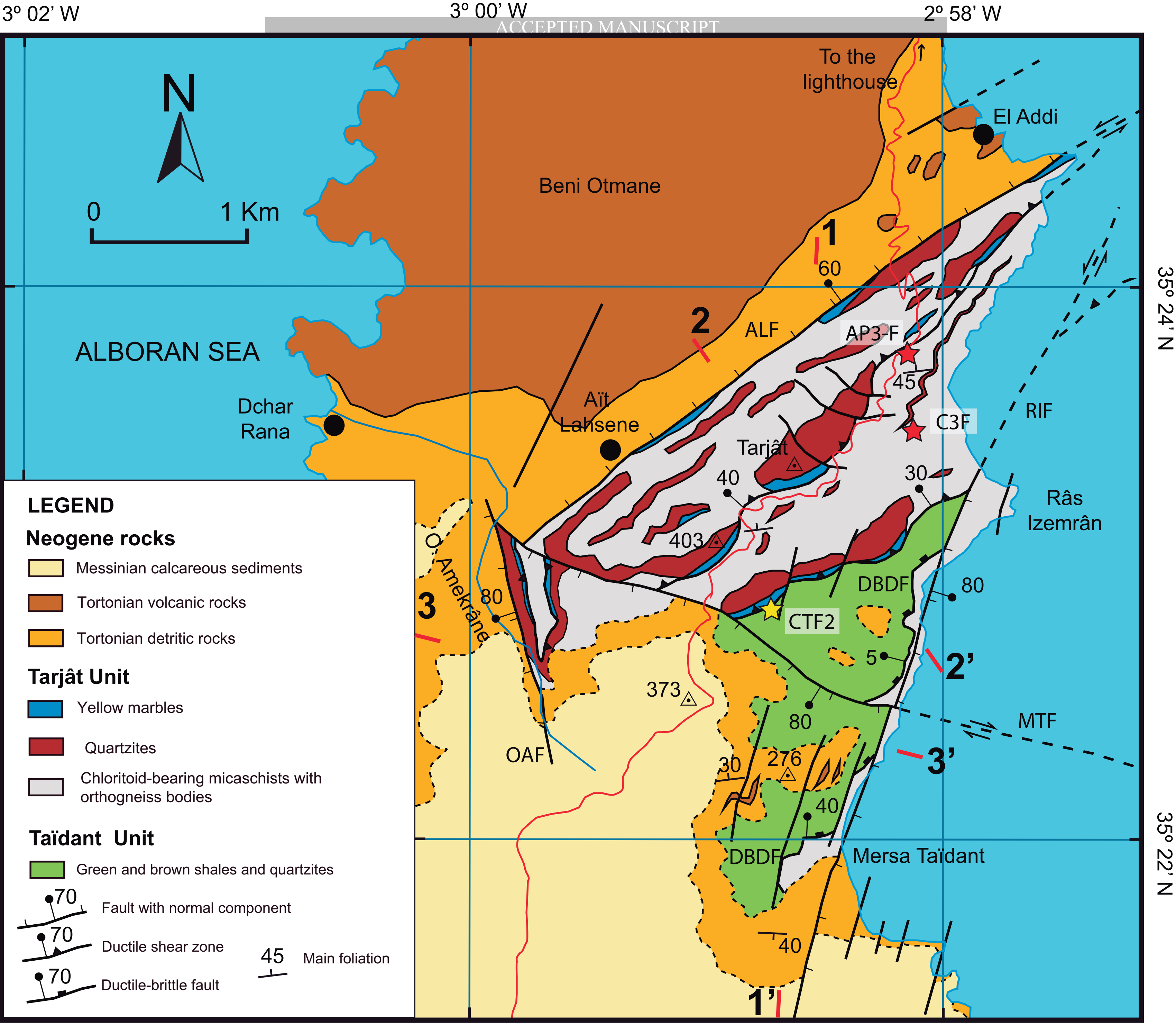
3º 02' W
3º 00' W
2º 58' W
35º 24' N
35º 22' N
N
0
1 Km
ALBORAN SEA
Beni Otmane
To the lighthouse
El Addi
Dchar Rana
Aït Lahsene
Tarjât
ALF
AP3-F
C3F
CTF2
RIF
Râs Izemrân
DBDF
MTF
OAF
O. Amekrâne
Mersa Taïdant
1
2
3
1'
2'
3'
60
45
40
30
80
5
403
373
276
LEGEND
Neogene rocks
Messinian calcareous sediments
Tortonian volcanic rocks
Tortonian detritic rocks
Tarjât Unit
Yellow marbles
Quartzites
Chloritoid-bearing micaschists with orthogneiss bodies
Taïdant Unit
Green and brown shales and quartzites
70
Fault with normal component
Ductile shear zone
Ductile-brittle fault
45
Main foliation

Figure 3

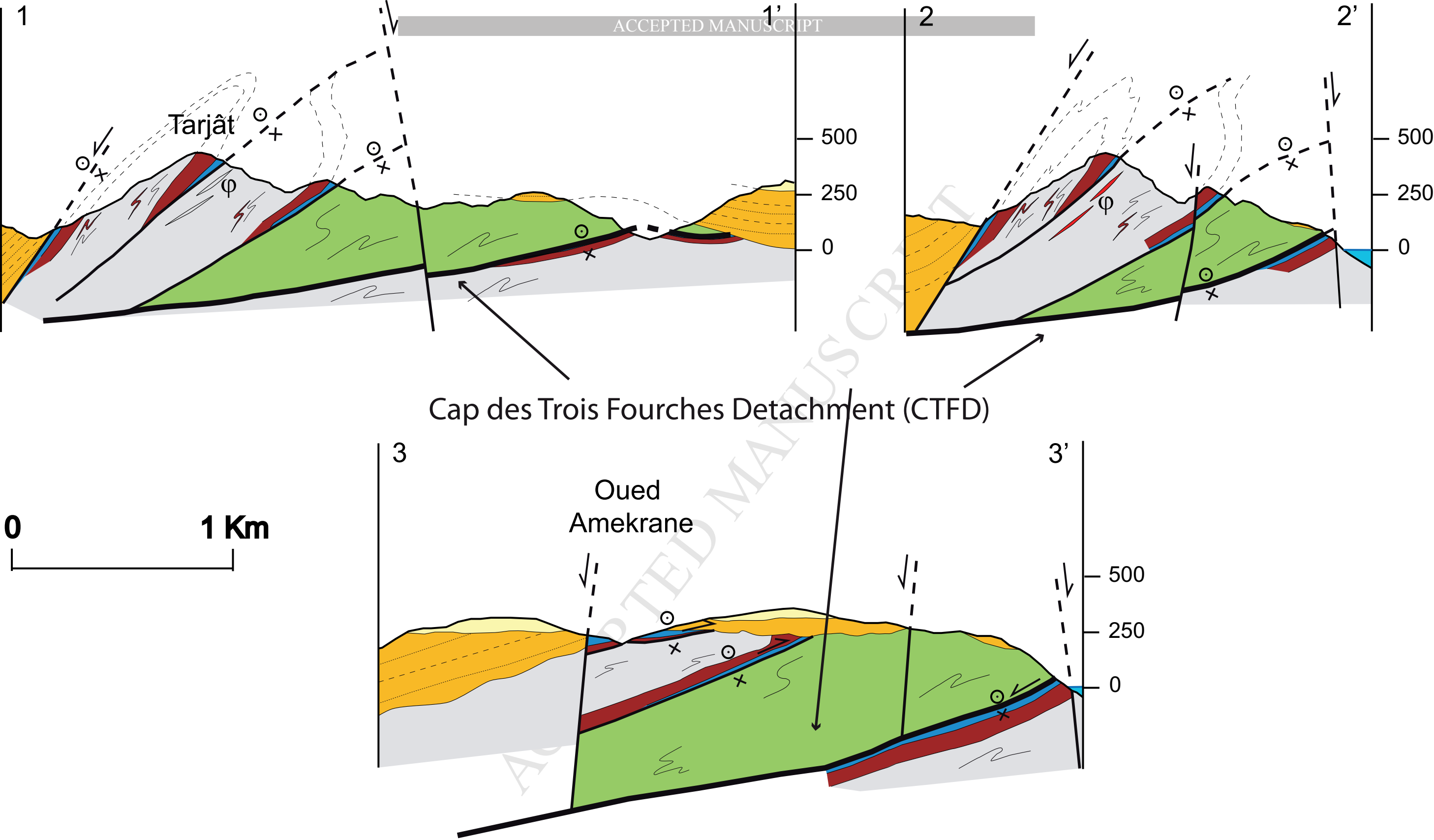

1
1'
Tarjât
φ
500
250
0
2
2'
500
250
0
φ
Cap des Trois Fourches Detachment (CTFD)
3
3'
Oued
Amekrane
500
250
0
0
1 Km

Figure 4

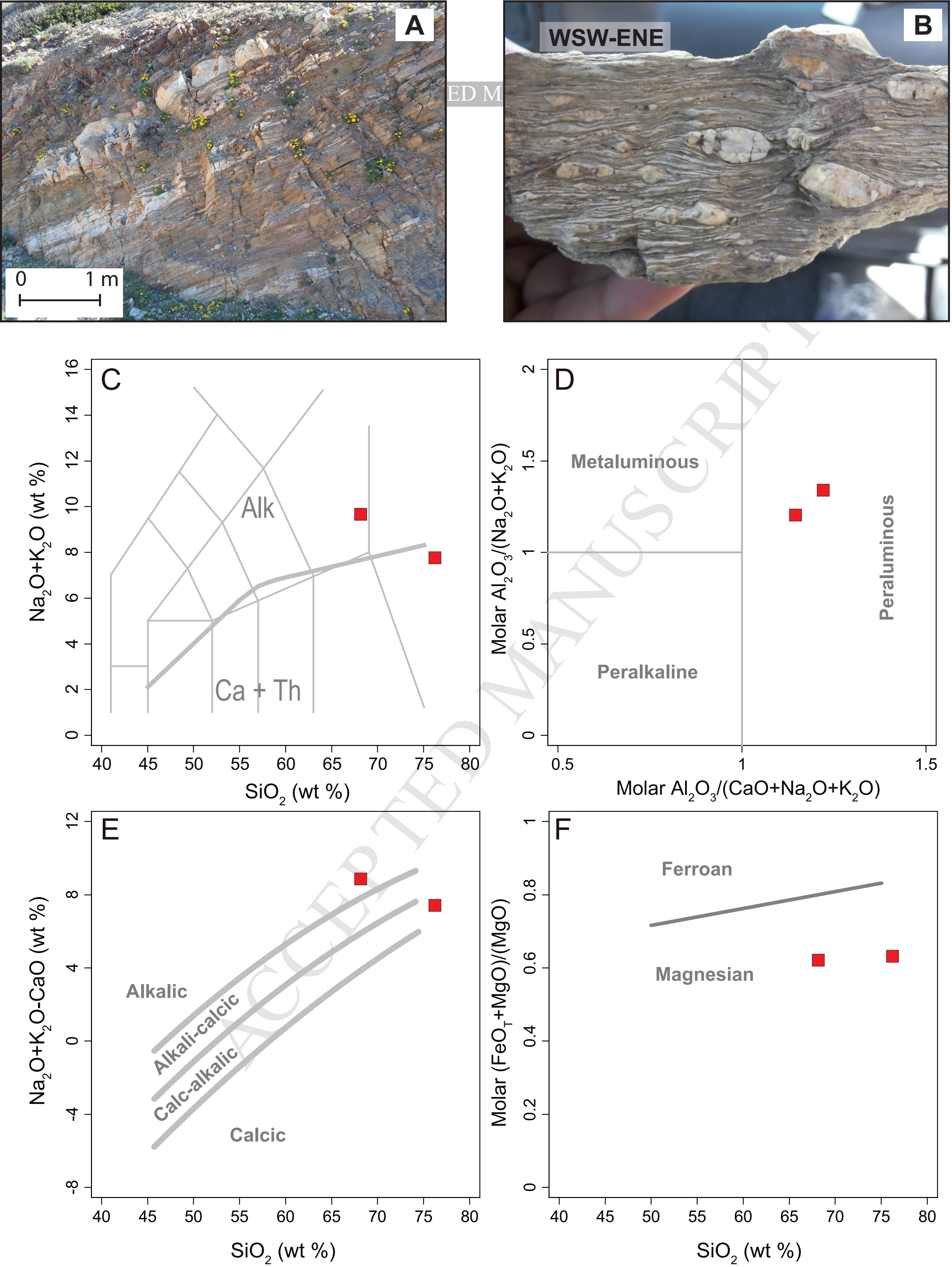
A
B
WSW-ENE
0
1 m
C
Na_2O+K_2O (wt %)
SiO_2 (wt %)
Alk
Ca + Th
D
Metaluminous
Peraluminous
Peralkaline
Molar $Al_2O_3/(Na_2O+K_2O)$
Molar $Al_2O_3/(CaO+Na_2O+K_2O)$
E
Alkalic
Alkali-calcic
Calc-alkalic
Calcic
Na_2O+K_2O-CaO (wt %)
SiO_2 (wt %)
F
Ferroan
Magnesian
Molar $(FeO_T+MgO)/(MgO)$
SiO_2 (wt %)

Figure 5

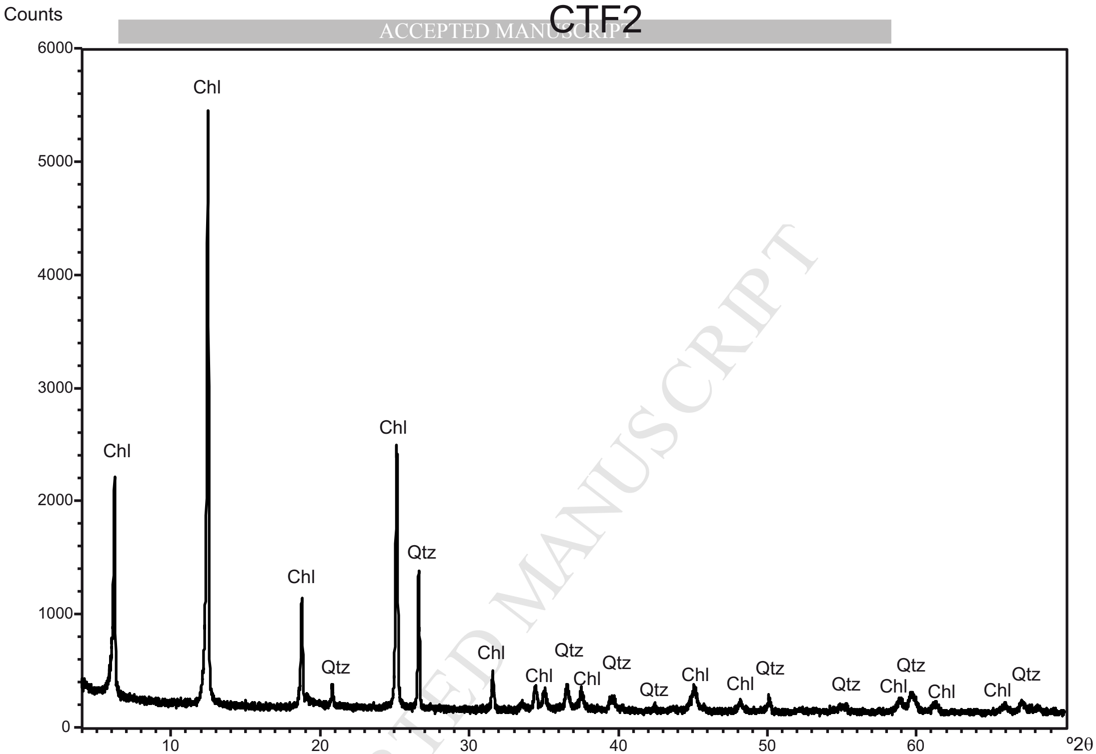
CTF2
Counts
6000
5000
4000
3000
2000
1000
0
10
20
30
40
50
60
º2θ
Chl
Chl
Chl
Chl
Qtz
Qtz
Chl
Qtz
Chl
Chl
Qtz
Qtz
Chl
Chl
Qtz
Qtz
Chl
Qtz
Chl
Chl
Chl
Qtz

Figure 6

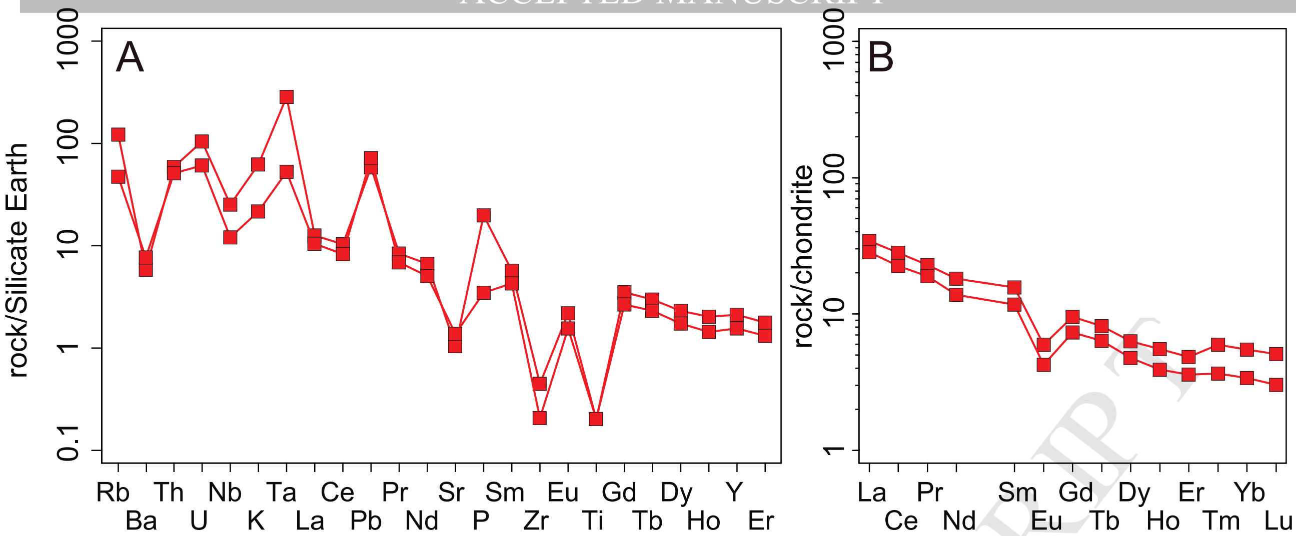
A
rock/Silicate Earth
0.1
1
10
100
1000
Rb Th Nb Ta Ce Pr Sr Sm Eu Gd Dy Y
Ba U K La Pb Nd P Zr Ti Tb Ho Er
B
rock/chondrite
1
10
100
1000
La Pr Sm Gd Dy Er Yb
Ce Nd Eu Tb Ho Tm Lu

Figure 7

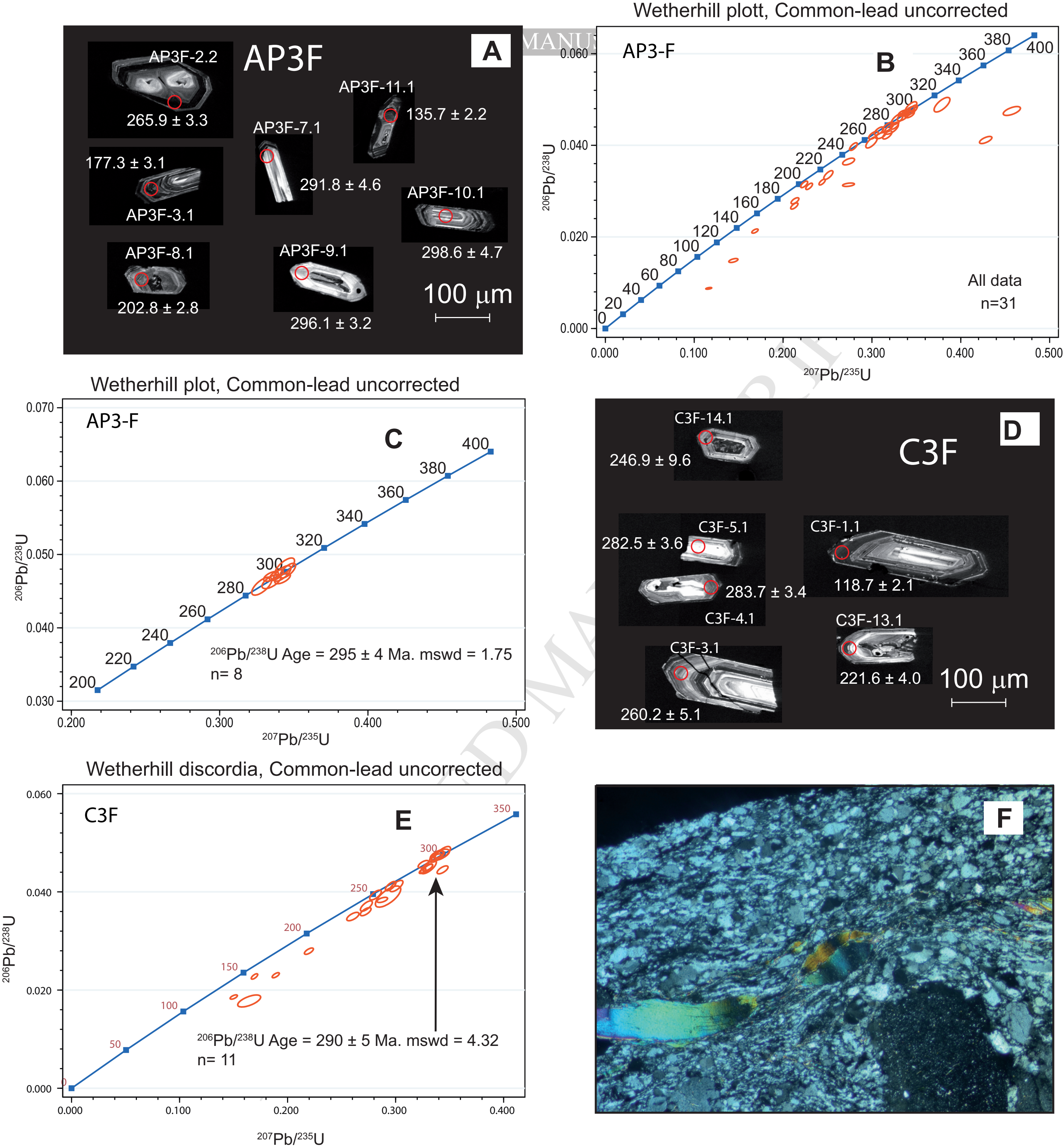

AP3F
A
AP3F-2.2
265.9 ± 3.3
AP3F-11.1
135.7 ± 2.2
AP3F-7.1
291.8 ± 4.6
177.3 ± 3.1
AP3F-3.1
AP3F-10.1
298.6 ± 4.7
AP3F-8.1
202.8 ± 2.8
AP3F-9.1
296.1 ± 3.2
100 μm
Wetherhill plott, Common-lead uncorrected
AP3-F
B
All data
n=31
$^{206}Pb/^{238}U$
$^{207}Pb/^{235}U$
Wetherhill plot, Common-lead uncorrected
AP3-F
C
$^{206}Pb/^{238}U$ Age = 295 ± 4 Ma. mswd = 1.75
n= 8
C3F
D
C3F-14.1
246.9 ± 9.6
C3F-5.1
282.5 ± 3.6
C3F-1.1
283.7 ± 3.4
118.7 ± 2.1
C3F-4.1
C3F-13.1
C3F-3.1
221.6 ± 4.0
260.2 ± 5.1
100 μm
Wetherhill discordia, Common-lead uncorrected
C3F
E
$^{206}Pb/^{238}U$ Age = 290 ± 5 Ma. mswd = 4.32
n= 11
F

Figure 8

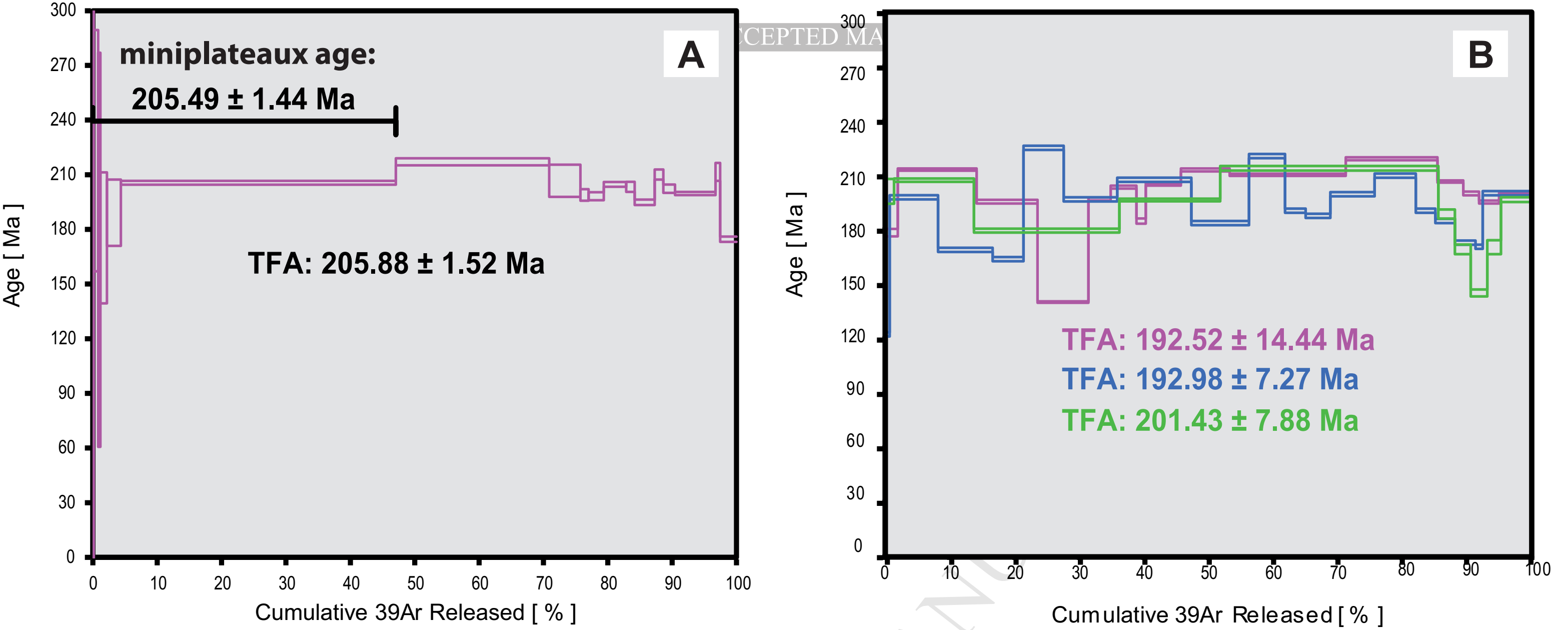
A
miniplateaux age:
205.49 ± 1.44 Ma
TFA: 205.88 ± 1.52 Ma
Age [Ma]
Cumulative 39Ar Released [%]
B
TFA: 192.52 ± 14.44 Ma
TFA: 192.98 ± 7.27 Ma
TFA: 201.43 ± 7.88 Ma
Age [Ma]
Cumulative 39Ar Released [%]

Figure 9

We determined the structure of the Cap des Trois Fourches area

We describe, for the first time, the orthogneisses in the area ages

U-Pb SHRIMP zircon geochronology yield early Permian ages for their protoliths

We propose a model of the crustal structure